ASD-TR-61-338
Part II

FATIGUE IN SHEAR BY BENDING OF STRUCTURAL SANDWICH CONSTRUCTIONS

TECHNICAL REPORT NO. ASD-TR-61-338, PART II
MARCH 1963

DIRECTORATE OF MATERIALS AND PROCESSES
AERONAUTICAL SYSTEMS DIVISION
AIR FORCE SYSTEMS COMMAND
WRIGHT-PATTERSON AIR FORCE BASE, OHIO

PROJECT No. 7381, TASK No. 738103

(Prepared under Contract No. AF33(657)-7309
by Northrop Corporation, Norair Division,
Hawthorne, California
D. R. Apodaca and J. L. Preston, Authors)

NOTICES

When Government drawings, specifications, or other data are used for any purpose other than in connection with a definitely related Government procurement operation, the United States Government thereby incurs no responsibility nor any obligation whatsoever; and the fact that the Government may have formulated, furnished, or in any way supplied the said drawings, specifications, or other data, is not to be regarded by implication or otherwise as in any manner licensing the holder or any other person or corporation, or conveying any rights or permission to manufacture, use, or sell any patented invention that may in any way be related thereto.

ASTIA release to OTS not authorized.

Qualified requesters may obtain copies of this report from the Armed Services Technical Information Agency, (ASTIA), Arlington Hall Station, Arlington 12, Virginia.

Copies of this report should not be returned to the Aeronautical Systems Division unless return is required by security considerations, contractual obligations, or notice on a specific document.

FOREWORD

This report was prepared under USAF Contract AF33(657)-7309 by the Structural Analysis Branch, Research and Technologies Section of the Northrop Corporation, Norair Division, Hawthorne, California. This contract was initiated under Project 7381, Task 738103 and was administered under the direction of the Directorate of Materials and Processes with Mr. F. H. Bair as project engineer. It was sponsored by the Aeronautical Systems Division, Air Force Systems Command, Wright-Patterson Air Force Base, Ohio.

All testing was performed at the Norair Engineering Test Laboratory. Acknowledgement is made to R. R. Spatz and B. J. Dixon for the excellent testing support, to E. K. Walker for assistance in analytical evaluations and to J. D. Revell, M.T.M. of Structure Analysis. This report covers work performed during the period 15 March 1962 through 15 January 1963. This contract was a continuation of the work carried out in the basic program under Contract AF33(616)-7200 reported as ASD-61-338. Contractor has assigned NOR 63-25 to this report for internal identification.

ABSTRACT

The Dynamic Test Method has been successfully applied for obtaining core fatigue in shear by reversed bending of a double cantilever beam sandwich specimen containing heavy tip-end masses. The testing approach consists of applying forced vibrations at resonant frequency with an electromagnetic shaker for each stress level desired. Reliable and reproducible S-N fatigue curves were produced on adhesive-bonded aluminum alloy and brazed stainless steel specimens containing representative shear test areas. The uniformity of the core cell geometry and quality of the interface bond were found to have a significant effect on the fatigue life of the sandwich construction. Problems associated with specimen support, shear and bending stresses, symmetrical balancing, stress concentrations, and transmissibility response were overcome through refinement of specimen configuration and test procedure.

PUBLICATION REVIEW

This report has been reviewed and is approved.

FOR THE COMMANDER:

W. P. Conrardy

W. P. CONRARDY
Chief, Materials Engineering Branch
Applications Laboratory
Directorate of Materials & Processes

TABLE OF CONTENTS

LIST OF ILLUSTRATIONS

<u>LIST OF TABLES</u>

I INTRODUCTION

Prediction of the behavior of structural sandwich constructions in a design is extremely complex because of the many variables associated with this material which enter into the problem. The problem is further complicated by the additional variations introduced by material quality and manufacturing processes which have an increasing detrimental effect on the service life of a structure. A large amount of theoretical data has been developed for static prediction of sandwich construction; but predicted results are usually significantly different from actual behavior, because of simplifying assumptions incorporated into the analyses. If an optimum design is to be obtained utilizing sandwich construction, a theoretical program supported by reliable test data is needed to ascertain the significant parameters involved. Many testing procedures now in common use lead to significant errors, even though the results appear to be consistent. So far only a few testing approaches have been developed which show promise for consistently developing accurate and reliable test data on the properties of sandwich constructions.

Static analysis of sandwich construction has been concerned primarily with general instabilities and boundary conditions, but it has not always considered fatigue behavior under dynamic loading conditions. The experimental work performed by the Northrop Corporation, Norair Division, using the Dynamic Test Method, has revealed many inherent weaknesses in sandwich constructions. These built-in weaknesses are responsible for early fatigue failures in service and must be corrected if increased fatigue resistance is to be realized in this form of construction.

The Dynamic Test Method was originally investigated by Northrop as a test approach for Young's and shear moduli because of questionable test results obtained by static test methods, Reference 1. Results of tests performed by the static method generally produced low but consistent moduli when local deflections at the loading pads were ignored. However, when the local effects were included, the computed moduli generally increased, but the scatter became prohibitive and the results inconclusive. Measuring small increments of static load and extremely small deflections requires highly sensitive instruments. In contrast, a frequency of 1500 cycles per second can be measured with standard equipment to within 0.1 percent when using the Dynamic Test Method. Calibration and measurement errors are minimized by expressing amplitudes in ratio form. The definition at resonant frequency is excellent because of the low damping coefficient of small sandwich specimens. A large load amplification is obtained when testing under forced vibrations at the resonant frequency as shown below.

* *

Manuscript released by the authors March 1963 for publication as an ASD Technical Report.

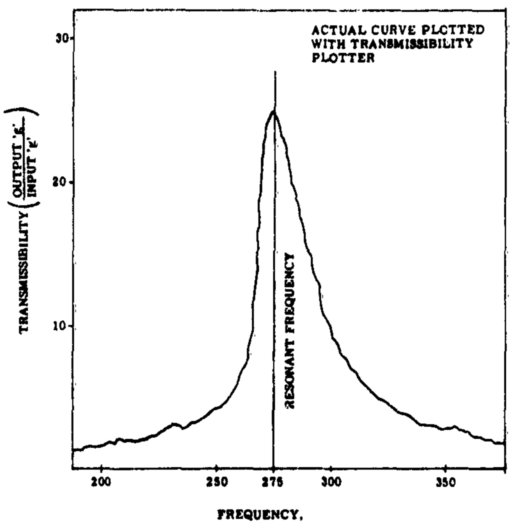

II SELECTION OF FLEXURAL MODE

The Dynamic Test Method was investigated as an approach to fatigue testing in tension-compression loading in the basic contract reported in Reference 2. With a few modifications, this method proved highly satisfactory as a short-time-testing procedure for fatigue determination of sandwich construction under dynamically balanced conditions. It was demonstrated that reliable and reproducible S-N fatigue curves could be obtained for brazed and bonded sandwich specimens.

Using the knowledge and experience gained during previous investigations, an extension of the basic contract was granted to determine whether the Dynamic Test Method could be adapted to the determination of core fatigue in shear through reversed bending-induced shear stresses. This mode is considered more representative of actual loading conditions encountered in service. A brief discussion of the three testing methods is presented in Reference 3.

To achieve the reversed bending-induced shear stresses in the core, a long narrow specimen forming a symmetrical double cantilever beam was selected from various approaches under consideration as specimen configuration. Excitation was accomplished with an electro-magnetic shaker through a single-point load path located at specimen midspan. Provisions were made for attaching heavy masses to both ends of the beam in order to develop the high shear stresses necessary to produce core fatigue within a frequency range of 200 to 300 cycles per second.

The specimen was allowed to vibrate in a completely reversed or sinusoidal mode at an amplitude determined to produce fatigue at the desired number of cycles. When fatigue was initiated in the specimen, the impressed force was correspondingly increased to compensate for the decrease in transmitted force and continued to final catastrophic failure.

III PROGRAM DEVELOPMENT

The early portion of this program was directed toward the development of a test configuration in the form of a simply-supported, double-cantilever beam with tip-end masses, which could be used to develop fatigue data through bending-induced shear. Parametric analyses were made to show the relationship between specimen length, shear loads, and face fiber stresses (Figure 1). From these analyses and preliminary tests, it was evident that a compromise had to be made between the specimen length and resonant frequency if representative shear test areas were to be developed and maintained. Specimens having a low ratio of facing-to-core thickness were found unsuitable because of excessive fiber stresses in the facing material resulting in fatigue failure at the faces. A specimen size was needed which would have a resonant frequency of 200 to 300 cps, contain a test area 3 to 5 inches long, and yet produce low bending moments. The beam would also have to be sufficiently wide - at least ten cells across - to provide a stable core foundation and representative shear area which would minimize the effect of defective or irregular core cells.

Initially the test specimens were fabricated along these guidelines, but detrimental stress concentrations and high fiber stresses continued in the facings despite the design of the midspan support. Accurate data was needed of the loads and test configuration required to promote shear fatigue in the core while avoiding failure in the faces. Shortening the specimen span length was considered, but this would have significantly reduced the length of the effective core shear area. The addition of reinforcement facings to the test specimens was ultimately found to be the most practical alternative. Aluminum was tried first but 17-7 PH (TH 1050) stainless steel was found to be far superior because of its exceptional fatigue strength.

Tests were performed for determining the effects of changes in weight of end-masses, laminations and additional stiffness created by reinforcement facings, and span length. The results of these tests are presented in Table 1 below and plotted in Figure 2. As evident in the results, the resonant frequency is sensitive to changes in span length, weight of end-masses, stiffness of the panel, and facing laminations. The increase in facing thickness resulted in an increase in the resonant frequency of both aluminum and stainless specimens, primarily due to the additional change in stiffness. A resonant frequency of approximately 200 cps was produced with masses weighing 3 pounds on each end. Without the use of these additional facings, it would have been impossible to maintain a representative shear test area and develop the desired resonant frequencies and core shear stress levels.

TABLE 1

EFFECT OF WEIGHT AND LOCATION OF END MASSES, WITH AND WITHOUT REINFORCEMENT FACINGS, ON THE RESONANT FREQUENCY

		Without Reinforcement		With Reinforcement (4)	
Wt. of Mass, lbs.	Distance (1) of Mass, in.	Resonant frequency, cps		Resonant frequency, cps	
		17-7 PH(2)	5052-H39(3)	17-7 PH(2)	5052-H39(3)
None	None	450.4	359.3	481.4	546.2
1.5	3	313.4	235.3	397.5	407.1
1.5	4	278.4	170.7	344.4	337.7
1.5	5	230.8	129.7	300.4	285.7
1.5	6	193.6	102.3	264.3	244.4
3.0	3	256.6	176.1	323.8	333.1
3.0	4	204.2	119.7	266.8	253.6
3.0	5	165.8	90.6	227.9	214.6
3.0	6	139.7	72.1	196.4	177.2

(1) Distance from center of support to center of each end mass on 3" x 14" specimens.
(2) Type g specimen - 7.5 pcf density 1/4 sq. 0.002P stainless, brazed.
(3) Type e specimen - 5.7 pcf density 3/16 hex. 0.002P aluminum, bonded.
(4) Both sides, bonded 17-7 PH (TH 1050), 0.060-in. thick.

IV DETERMINATION OF EFFECTIVE SHEAR AREA

In defining the zone within the flexure test specimen that would represent only bending-induced shear fatigue in the core, the specimen was assumed to consist of a cantilever beam subjected to forced oscillations at the attachment point and with the concentrated masses at the tips. Each zone, located between the midspan support and an end mass, must, however, be reasonably free of loading stresses other than those produced in shear. As the distance between the two concentrated masses is increased, the bending moments are proportionately increased, resulting in high fiber stresses and low resonant frequencies. Consequently, the span must be kept as short as practicable in order to minimize the effect of bending stresses; yet it must be long enough to maintain a representative shear area within each beam. However, when the specimen length is decreased and the concentrated masses approach each other, combined loads are developed which tend to minimize the effective shear area within each beam in the specimen. Thus, a compromise in beam length must be made in order to account for effect of both bending moments and concentrated loads. It was determined that each effective shear area should contain at least 100 core cells to produce representative shear fatigue by reversed bending as shown in Table 2.

TABLE 2

CALCULATED VALUES OF EFFECTIVE SHEAR AREA OF EACH CANTILEVER BEAM FOR DIFFERENT SPECIMENS

Specimen Type*	Core Depth, in.	Center-to-Edge Length, in.	Effective Shear Length, in.	Effective Shear Area, in^2	No. of Cells in Area
e	0.625	5 6 7	2 3 4	6 9 12	170 256 340
d	0.625	5 6 7	2 3 4	6 9 12	96 144 192
g	0.500	5 6 7	2.25 3.25 4.25	6.75 9.75 12.75	108 156 204

* Type e - 5.7 pcf density, 3/16 hex 0.002 P, 5052-H39 aluminum, adhesive-bonded
Type d - 7.9 pcf density, 1/4 hex 0.004 NP 5052-H39 aluminum, adhesive-bonded
Type g - 7.5 pcf density, 1/4 sq. 0.002 P, 17-7 PH (TH 1050) stainless, brazed

To accurately define the shear test area (area not affected by combined loads or loads other than shear) of each beam of the specimen, a core thickness, equivalent to a shear diagonal, was subtracted from the edge of the midspan support and the end mass. The remaining span length between the midspan support and end mass is considered the effective shear area within the specimen. Any damage occurring outside the effective shear area would not be representative of shear fatigue by bending.

V FEASIBILITY STUDIES - TEST CONFIGURATIONS

Six different test configurations were investigated before a satisfactory configuration was developed which could be used to produce S-N fatigue data. In this report, "test configuration" includes the specimen, end-masses, midspan support, reinforcement sheets and balancing bars. Each configuration is identified in alphabetical order as shown in Figures 3 and 4. The development of the test configurations was accomplished during Phase I of the program, Feasibility Studies. As anticipated, the effects of stress concentrations and concentrated bending moments caused premature failure of the specimens. This problem persisted throughout a greater portion of the program than had been anticipated, but Configuration F finally overcame this shortcoming. A brief discussion of each test configuration follows:

a. Configuration A

Configuration A, shown in Figure 3, was the first test arrangement investigated in this program. After a few unsuccessful tests, it became apparent that this arrangement contained too many weaknesses which produced early failure in modes other than fatigue in shear of the core. The stress concentrations, developed beneath the top midspan supports, were responsible for premature failure of the top face sheet after a short test duration. Another problem was the inertial stresses created by the heavy tip-end masses resulting in failure through crimping of the core. Also, crushing of the core resulted at the mass-attach bolt holes.

b. Configuration B

In an effort to solve the problems created by Configuration A, the end masses were partially located as inserts within the core area at each end of the beam, as shown in Figure 3. Upon testing, it became evident that the use of solid-inserts and the method of their attachment were not satisfactory because of longitudinal restraints created on the face sheets and shear restraints on the core during reversed bending. The configuration was further modified to the form represented by the following to allow freedom for bending displacements.

c. Configuration C

The modification incorporated in this configuration consisted of splitting the end-mass inserts across the neutral axis in order to allow free displacement in bending, Figure 3. To prevent tensile displacement or separation of the inserts, a thin rubber shim was bonded to the faying surfaces of the split halves. Overheating of the shims was caused by the rapid cyclic displacements of the insert halves resulting in failure of the bond. In an effort to correct this problem, an adhesive (EC 1675) was substituted for the rubber, serving as both the spacer and bonding agent. Again, failure occurred due to rapid heating at the ends. This resulted in expulsion of the heated adhesive and a rapid drop in transmissibility. Crushing of the core located by the inward edges of the masses occurred as a result of high inertial bending moments. This configuration was abandoned when it was determined that the inherent problems could never be satisfactorily resolved.

d. Configuration D

In an effort to resolve the problems associated with shear restraint and stress concentrations created by the end masses, liquid mercury was used to provide the end masses. One pound of mercury was injected through small holes located on the top face sheet into 116 core cells at each end of the specimen. Although this method proved very effective for short test durations, containment and rapid heating of the mercury accompanied by high damping became a problem. Corrective efforts were unsuccessful because of the high dynamic pressure produced and corrosive nature of the hot mercury. This approach was investigated on both, aluminum and stainless steel sandwich specimens, but was later completely abandoned.

e. Configuration E

The problem of high facing stresses resulting in premature failures had been minimized by using thicker face sheets on the specimens in Configuration D, but this problem persisted after testing for extended duration. In order to develop and maintain high shear stress levels on the core material it was mandatory that the detrimental effect of stress concentrations and facing stresses be either circumvented or eliminated. An approach investigated for circumventing the effect of stress concentrations consisted of bonding a reinforcement sheet over each face sheet. The end masses were bonded over each end of the reinforcement sheets, as shown in Figure 4. Both aluminum and stainless steel reinforcement sheets were tried, but failure by cracking persisted on the face sheets about one-half inch inward from the reduced edge of the midspan support. Observation of the displacement of the specimen and edges on the supports during excitation revealed a slight but significant bridging effect produced between the support and specimen. The cause of bridging is attributed to the difference in the stiffness of sandwich materials as compared to the support. To correct this condition would require machining a close-tolerance exponential curve on each support compatible with bending deflections of each material tested - a task considered not only impractical but also prohibitive in cost. The design of the midspan support fixtures was changed and the reinforcement sheets were modified on the following test configuration.

f. Configuration F

The heat treat strength and thickness of the 17-7 Ph reinforcement sheets was increased from Condition A to TH 1050 and from 0.020-inch to 0.060-inch, respectively. The weight of the masses at each end was changed to 3 pounds per end. The midspan support fixtures were machined from a square steel bar to provide the smallest possible contact area of 1/2" x 3" yet maintain structural rigidity. A thin asbestos gasket was located between each support fixture bar and the specimen in order to provide a uniform contact area during reversed bending and to prevent metal-to-metal contact. No attachments were made through the test specimen, shifting during excitation being prevented by the bolts located through the tabs on the top reinforcement sheet. This also accomplished attachment between the top and bottom midspan supports. With a few refinements, this configuration proved very effective and all test data subsequently developed was accomplished using it. A detail drawing of the reinforcement facings and masses is presented in Figure 5.

VI EFFECT OF MIDSPAN SUPPORT

The midspan supports used in test Configurations A through E were made of steel for the stainless specimens and aluminum for the aluminum specimens, but were similar in shape. Each side had a geometrical curvature designed to sustain a uniform stress pattern in the specimens at midspan as they were caused to bend during the reversed bending action. The graduated spring action was obtained by a progressive reductio n in thickness of the supports from the center toward the edges (See Figure 3). At high frequencies, sliding friction resulted in a progressive rise in temperature between the specimen and the supports, despite the ample use of dry lubricants. High bending moments produced premature failure at the facings due to the stress concentrations. Fatigue cracks at the facings developed beneath the supports after short test durations even after the strength and thickness of the facings had been increased.

The design of the midspan supports was changed in Configuration F in an effort to avoid premature failure of the facings. Attachment of the specimen at midspan was also revised so that bolts were no longer located through the specimen but on the sides of the specimen through tabs provided on the top reinforcement facing. Thus, the smaller contact area at midspan provided a minimum support as explained in Section V-f above, and this arrangement was ultimately adopted for developing the fatigue data presented in this report.

VII "CALIBRATION" OF TEST SPECIMENS

Establishment of the proper transmissibility (ratio of transmitted to impressed forces) for sandwich specimens forming a double-cantilever beam was, during a great portion of the program, a very serious and perplexing problem. The transmissibility of identical specimens varied considerably, even for those taken from the same panel. At that time, it was believed that specimens exhibiting low ratios were of poor quality since failure often occurred after a relatively short test duration. Conversely, specimens that exhibited high ratios usually lasted for a proportionately greater test duration. Close observation of specimen response during a series of tests conducted on identical test specimens revealed that the transmissibility was not wholly dependent on the quality of the specimen, but was primarily dependent on the method of attachment and tightness to the midspan support. Sine waves produced by these conditions were observed and recorded on photographs which showed a distinct difference in shape for identical specimens as shown below.

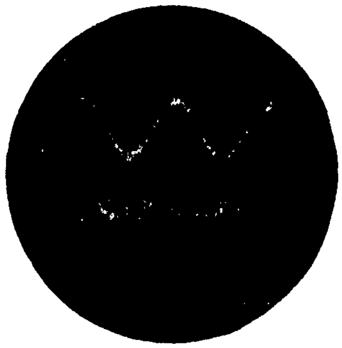

INPUT LOAD 21"g" (LOWER CURVE)
OUTPUT LOAD 90"g" (UPPER CURVE)
RESONANT FREQUENCY 185 CPS
LIFE 234,000 CYCLES

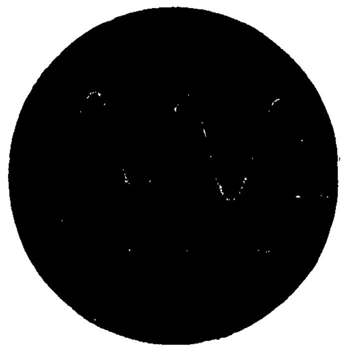

INPUT LOAD 0.8"g"
OUTPUT LOAD 90"g"
RESONANT FREQUENCY 194 CPS
LIFE 1,000,000 + CYCLES

On the basis of this finding, a curve was plotted showing the output "g" load (transmitted forces) versus the input "g" load (impressed forces) as affected by the method of attachment and tightness to the midspan support as shown below. A linear relationship was obtained which existed up to some point where deviations were obtained but at different values, depending on the adjustment and tightness of the specimen as shown below. Thus, it was obvious that it would be necessary to "calibrate" each specimen with respect to a characteristic curve, if accurate and reliable test results were to be obtained.

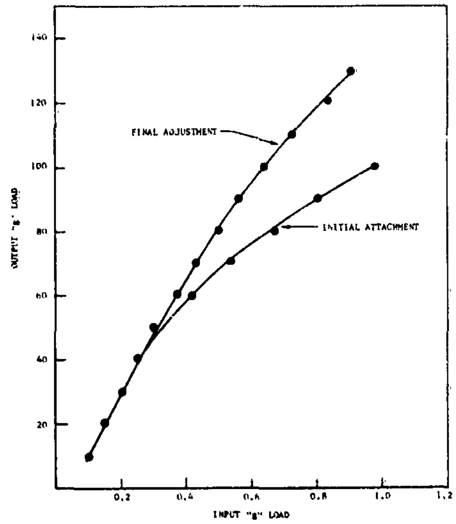

The procedure adopted for calibrating each specimen in a series consisted of making plots of output-to-input "g" loads at increasing ratios and different adjustments and tightness until the maximum obtainable transmissibility curve was produced. If this curve was identical to the one derived from the reference specimen (a specimen used only for checking the transmissibility characteristics of a panel from which the test specimens were obtained), then testing was initiated at the desired shear stress level. However, if the curve deviated prematurely, the specimen was readjusted, retightened, and a new transmissibility curve plotted. Before fatigue testing was started, the transmissibility of the specimen was first checked until a curve identical to the one derived from the reference specimen was obtained.

After final adjustment had been made, the maximum point at which deviation from linearity occurred was considered to be the maximum amplitude at which to test because testing above this point can easily damage the specimen. Once calibration of a specimen was accomplished, the desired shear stress level for the specimen was adjusted on the basis of the output "g" loads.

To verify the validity of "calibration" used in this approach, a series of tests were performed on a solid aluminum plate to check if the response of the solid plate was similar to the response of the sandwich panels. It was learned that, although the transmissibility of the solid plate was considerably higher than that obtained for the sandwich panels, the overall transmissibility characteristics and response were identical for both materials, including deviation from linearity and effect of adjustment and tightness of the specimen to the midspan supports.

VIII DYNAMIC BALANCING OF SPECIMENS

Dynamic balancing of the double cantilever beam was accomplished primarily by careful positioning of tip-end masses, reinforcement facings, and location of the specimen. No problems were encountered in maintaining a symmetrical and balance motion between the two free beams of the specimen. Although two small adjustable masses were located over the tip-end masses to establish dynamic balance in the system, they were not considered mandatory, for the most part, because the three-inch width of the specimen alone provided adequate balance. Although each accelerometer was located at a point along the center-line of the specimen, g-load readings at the side edges of the masses were rarely taken because the difference in response was so small that the extent of experimental error by any twisting motion was considered negligible.

IX TERMINATING A TEST

Failure of a sandwich specimen under forced vibrations at resonance is normally accompanied by a gradual decrease in resonant frequency and a rapid drop in transmissibility (output-to-input acceleration ratio). Any change in the condition of a test specimen results in a change in the spring constant (stiffness) of the structure. Initially, a five percent shift in the resonant frequency was used as the criterion for stopping a test. Several test specimens containing little or no discernible fatigue damage were prematurely destroyed using this criterion. Because the interval between fatigue initiation and final failure is short, it was decided to stop the test when final failure (complete drop in transmissibility) occurred. The life of the specimen is very short during this interval, and constitutes only a small percentage of the total number of cycles from test initiation until final failure (Figure 6). This condition is true, however, only when the impressed force is proportionately increased to maintain the same output "g" acceleration throughout the entire test period. The interval during which failure progresses is generally accompanied by a high pitch noise emanating from within the specimen.

Visual examination of the exposed core cells did not reveal the point at which failure was initiated, as had been anticipated. Even with the aid of a strobe light, fatigue damage in these areas was difficult to differentiate from other surface defects.

X DETERMINATION OF FATIGUE DAMAGE

Determination of the exact location of fatigue crack initiation in sandwich construction is very difficult due to the complex geometry of the core material. The general criterion that fatigue-fractured surfaces contain chevron or beach marks is of little value when examining thin foil material within a maze of core cells. In the tests conducted, the damaged area within the core generally consisted of hundreds of cracks, and this quantity was independent of the magnitude of the stress level or the number of cycles to failure. The fact that damage occurred due to stresses other than shear, further complicated the problem of determining the extent of fatigue damage.

The specimens were maintained under forced vibrations at the same transmitted force level during the entire interval between test initiation and test termination. Between fatigue initiation and final failure a loss of structural integrity of the test specimen was evidenced by a torsional oscillatory motion. Damage caused by this additional mode was in some cases quite severe, particularly at the outer cells in the specimen. It can, however, be isolated from fatigue damage by comparing the failure modes at the edges to those within the core. Additional damage was caused when the face sheet was peeled off to examine the nature and extent of damage within the core. The principal criterion used to distinguish fatigue from other damage was the presence of characteristic multiple cracks which are peculiar to fatigue damage only. This is discussed in the following section.

XI FATIGUE FAILURE MODES

Fatigue in shear on both, aluminum alloy and stainless steel sandwich specimens, was repeatedly reproduced in the effective shear zones of the specimen between the midspan support and the end masses. The mode of failure was, however, decidedly different for each material. In both cases, fatigue damage was generally more pronounced on the top side of the specimen than on the bottom, due, perhaps, to the additional effects of gravity on the end masses.

On aluminum panels with 0.004-inch ribbon, multiple fatigue cracks were initiated at the edges of the core ribbon beneath the adhesive on both sides of the specimen and adjacent to the corner junctions or nodes of the cells as shown in the sketch below. These cracks, usually appearing in pairs, propogated normal to the faces and joined at about one-eighth inch from the point of initiation. The area surrounded by the cracks was loosened by the vibrations and expelled from location. Secondary cracks were subsequently initiated at the radius formed by the primary cracks. A considerable amount of debris was accumulated in the failure zones, as shown in the photograph of Figure 7a.

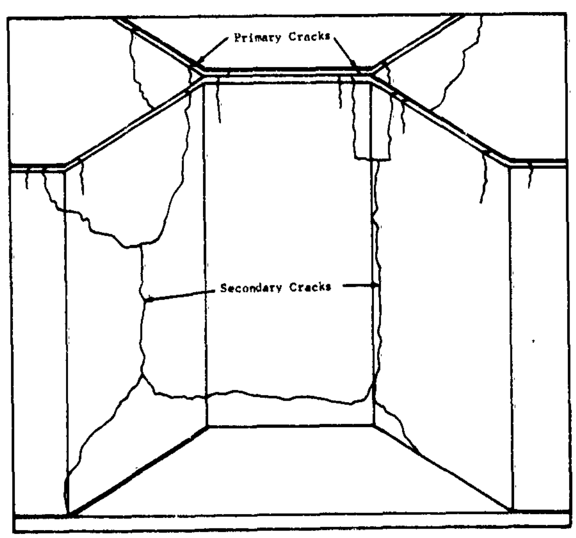

On the aluminum panels with 0.002-inch foil, the failure mode was similar to that for the thicker foil, except that the primary cracks propagated a greated distance before joining with other cracks. A photograph of the failed zone is presented in Figure 7b.

On the stainless steel panels single and, in many instances, double cracks were initiated in the flat area of the core cells about mid-height of the core. The cracks produced by fatigue usually propagated at a 45 degree angle to the panel thickness. An "x" was developed in areas where two cracks formed on the same flat area as shown in the sketch below. Only a small amount of debris was found in the specimen after final failure as shown in the photograph of Figure 7c. Usually failure was more pronounced on one beam in the specimen than on the other and, in some cases, no failure was evident at all on one of the beams.

The mode of failure exhibited by the stainless steel specimens was unique in that the majority of the fatigue cracks were initiated within the flat surfaces of cell ribbon. These cracks are representative of expected shear failure, i.e., 45 degrees to the specimen height. Some of the cracks propagated a short distance, then stopped approximately one-sixteenth inch from the interface braze fillets. Only a small percentage of cracks propagated through the perforation holes in the core cells. It appears that the coining produced during punching of the perforation holes determined whether the cracks would initiate at the holes or propagate around them. The mode of failure is such that the fatigue cracks will develop in these areas, regardless of the presence or absence of perforations.

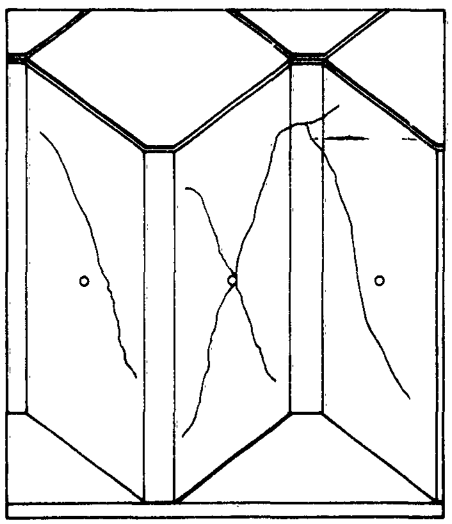

XII EFFECT OF REINFORCEMENT FACINGS

When a sandwich specimen is excited at resonant frequency as a double-cantilever beam with heavy concentrated masses at the tip-ends, the bending moments are resisted primarily by the facings, while the shear stresses are absorbed, for the most part, by the core and face-to-core bonding material. During the greater portion of this program stress concentrations which were produced at critical locations in the facings resulted in premature failure before fatigue in shear could be developed in the core. In order to retain a representative shear test area, the strength and/or thickness of the facings had to be increased to preclude facing failures. Increasing the thickness of the facings by bonding an additional reinforcement sheet to each side of the specimen was tried and found to be a satisfactory alternative. These additional facings not only minimized the effect of stress concentrations and fiber stresses, but also increased the rigidity of the specimen, and hence, the resonant frequency.

It was evident, however, that the resultant change produced by the thick, strong facings had to be included in the analysis if the true core fatigue strength of the core in shear was to be determined. Two methods were available for determining the shape factor of the specimen resulting from the change in specimen facing thickness and spring constant and are presented in Appendix A. The first method accounts for the change in shape factor by Q/I, and the second accounts for the change in dynamic response. Utilizing these two methods - one for static analysis, the other for dynamic response - affords a method for cross-check of the results and an approach for determining those variables significantly affecting the results. Correlation of results obtained by the two methods was excellent, thus the change in the calculated Q/I by the addition of reinforcement facing was verified through the change in dynamic response. This correlation was encouraging as it had been impossible to include the viscous damping effect of the adhesive between the reinforcement facings and test specimen. Northrop unpublished test data had indicated that the adhesive was insensitive to viscoelastic effects at low frequencies. Results of tests confirmed this because the adhesive was shown to be insensitive and did not affect the test results.

By obtaining the change in dynamic response of a specimen - with and without reinforcement facings - the effective mass of the reinforcement facing can be computed with an equation presented in Section 6 of Appendix A. The increase in effective mass due to the reinforcement sheets was included in the calculation of the shear stresses.

The dynamic flexural test method lends itself to determining the shear modulus of the core. This is accomplished by varying the panel facing thickness and determining the change in resonant frequency. Since the dynamic spring constant is inversely proportional to the bending and shear deflections, the known change in bending deflections, the relative change in shear deflections, and the observed change in frequency can be used to determine the shear modulus.

XIII EFFECT OF IRREGULAR CELL GEOMETRY

Results of tests on Type d aluminum alloy specimens (5053-H39, 1/4 hex 0.004P) with areas containing irregular core cells ranging in shape from hexagonal to rectangular produced fatigue after short test durations. Failure was produced after only 5 x 10^4 cycles at stress levels designed to produce fatigue between 10^5 and 10^6 cycles. It was determined that the presence of stress concentrations due to cell irregularities was responsible for failures occurring prematurely. These irregularities give rise to localized stress concentrations which can, in turn, cause a significant reduction on the fatigue strength of the core. Based upon these findings, the uniformity of the core cells has a very significant effect on the fatigue life of sandwich constructions when dynamically loaded in shear by reversed bending. This effect was evident on all the specimens containing irregular core and/or defective cells.

XIV EFFECT OF ERRATIC BONDING

A series of tests were performed on test specimens fabricated from sandwich panels produced by the Boeing Company under Contract No. AF33(616)-8002, reported in ASD-TDR-62-631, Reference 4. These panels were furnished by ASD for fatigue evaluation by the dynamic flexural method in this contract. The panels consisted of three alloys, 17-7 PH (RH 950), PH 15-7 MO (RH 950) and HS-25 (annealed), each with dimensions of 19 x 21 inches. The panels were bonded at Boeing by a Boeing-developed technique consisting of a ceramic adhesive-braze alloy combination.

The fatigue specimens were fabricated with the ribbon direction remaining parallel to the length of the specimen. After the resonant frequency had been determined, an attempt was made to determine the transmissibility characteristics of the specimens. In all cases the response of the specimens was erratic resulting in a gradual decrease in the resonant frequency and a rapid drop in transmissibility. No specimen was found satisfactory for fatigue evaluation. Examination of the core in the specimens revealed defects in the brazements most of which were due to a lack of bond and fillet formation, and large accumulation of braze material in certain areas. As had been determined on other bonding materials, the quality of the bond was responsible for early failure. A poorly bonded structure is extremely sensitive to reversed bending stresses at high resonant frequencies. This applies to both, adhesive-bonded and brazed specimens.

XV DISCUSSION OF RESULTS

This program was concerned with fatigue properties in the longitudinal direction only (ribbon direction remaining parallel to the length of the specimen). A complete description of the sandwich materials used in the test specimens is given in Table 3. Although tests were performed on all types listed, valid and usable fatigue test data were developed only for specimens of Types d, e, and g.

a. Feasibility Studies

Results of fatigue tests conducted during the Feasibility Study portion of the program are presented in Table 4. Appropriate remarks are given after each entry denoting the results or purpose of the test. None of these data was used in the final analysis or plotted as S-N curves, although some of the results after specimen No. 12 are valid and conform to the trends exhibited in the fatigue curves. The main reason for not using these results is that the method used for "calibrating" the specimens for transmissibility characteristics had not yet been determined. All of these data, however, was used for establishing guidelines in the development of test techniques for each material subsequently tested.

b. Aluminum Alloy, Type d Specimens

Presented in Table 5 and plotted in Figure 8 are the results of tests conducted on adhesive-bonded aluminum alloy test specimens, Type d. The core material was 5052-H39 with 1/4-inch cell size and 0.004-inch ribbon thickness. Although fifteen specimens were tested, valid test results were obtained from only three. The many failures were due to final problems in the refinement of the technique and erratic core cell geometries. Some of these problems include bond failure between panel and reinforcement facings, determination of stress levels, overload, and misinterpreted failure occurrence.

c. Aluminum Alloy, Type e Specimens

Results of tests conducted on Type e specimens, adhesive-bonded aluminum alloy, are given in Table 6 and are shown plotted in Figure 9. The core material was 5052-H39 with 3/16-inch cell size and 0.002-inch ribbon thickness. Twelve valid tests were conducted on this material during this series of tests. A characteristic S-N fatigue curve was obtained showing increasing fatigue life at decreasing stress levels. Although some scatter in results is noted, the maximum distribution of strength is only 50 psi which is considered small in view of the complex nature of sandwich construction. The fatigue strength at 10^6 cycles is approximately 140 psi in shear or 27.0 percent of the reported (510 psi average) core shear strength determined by flatwise flexure tests (Reference 5).

d. Stainless Steel, Type g Specimen

Results of tests on 17-7 PH (TH 1050) Type g specimens, Solar-brazed 1-C series, are given in Table 7 and are shown plotted in Figure 10. The core material was 17-7 PH with 1/4-inch square cells and 0.002-inch ribbon thickness. The trend in this series of tests was exceptionally consistent, except for specimens 2 and 12, on which a difference of 52 psi was obtained at approximately 6×10^5 cycles. The fatigue life for different stress levels was predicted very closely due to the quality of the bond and uniformity of the core cells. Based on the results, the fatigue strength in shear, as determined by cyclic bending after 10^6 cycles, is about 170 psi or 20 percent of the reported (859 psi average) core shear strength derived from flatwise flexure tests (Reference 6).

The fatigue properties of this material under tension-compression loading are presented in Figure 11. These test data were produced during the basic fatigue program reported in Reference 2. Although agreement of data was good, a maximum scatter of about 100 psi is noted due, perhaps, to variations of the loading mode rather than the quality of material. The fatigue strength at 10^6 cycles, as interpreted from the curve, is approximately 315 psi or 14 percent of the average flatwise tension strength of 2200 psi (Reference 7).

XVI VERSATILITY OF THE TEST METHOD

The Dynamic Test Method described in this report can be adapted to testing several different materials and configurations. The electro-magnetic shaker and control system allows a wide range of testing parameters, so as to accommodate a variety of specimen geometries and test conditions. This equipment versatility and the short test durations required result in a reliable low-cost testing technique.

With a few modifications to the test specimen the flexural test approach presented in this report can be easily adapted to testing under simulated service conditions and frequencies. The use of high testing frequencies allows short-time testing procedures that are advantageous, not only in terms of cost, but also in terms of schedule considerations. As in other unit test approaches, the value of the results is related to the size and geometry of the test specimen.

XVII INSPECTION OF TEST SPECIMENS

Since X-ray inspection is not suitable for use on adhesive-bonded sandwich panels, the quality of the bond was initially determined with an ultrasonic instrument known as a Fokker Bond Tester. This instrument uses a vibrating transducer to correlate the elastic response of the adhesive to the quality of the bond. Because results from the instrument were sometimes misleading, it was decided to discontinue this practice and to rely on the ability of the laboratory to produce high quality panels. X-ray reports accompanying the stainless steel panels, furnished by ASD, showed that these panels contained satisfactory bond and fillet formation. Visual examination of the core after testing confirmed this report.

After test completion, the extent and mode of damage produced in the core was determined by removal of one of the faces in the test specimen. Although additional damage was incurred on the core during peeling of the face sheet, this method of inspection was found to be the only satisfactory method for examining the core.

XVIII SPECIMEN PREPARATION

All aluminum sandwich panels used in this program were assembled and bonded at the Norair Material Sciences Laboratory while the stainless steel sandwich panels were supplied by the ASD as GFE items. The bonding of the tip-end masses to the reinforcement sheets and subsequent bonding of the reinforcement sheets to the test specimens was accomplished by Material Sciences Laboratory personnel.

All test specimens were cut to dimension from the panels with the ribbon direction remaining parallel to the length of the specimen. The aluminum specimens were cut with a conventional table saw, and the edges of the facings deburred. The stainless specimens were cut with a band saw, and the edges were ground smooth and deburred. The width of the specimen was maintained at exactly three inches which, in many cases, resulted in broken cells along the edges. The broken cells had no noticeable effects upon the transmissibility of the aluminum specimens but did affect the stainless steel specimens by rubbing of the edges. This condition was corrected by separating the edges.

a. Preparation of Aluminum Sandwich Panels

1. Face Sheets

(a) Vapor degreased
(b) Etched in sulphuric chromate at 150 F for ten minutes
(c) Water rinsed and dried
(d) Sprayed with BR 227 to approximately 0.0005" thick
(e) Pre-cured at 240 F for thirty minutes

2. Sandwich Core

(a) Vapor degreased

3. Applied FM-61 or FM-48 adhesive to both core and face sheets

4. Cured under 60 psi pressure (55 psi applied load and 11" Hg vacuum) at 340 F for 60 minutes in an autoclave. Note: Temperature raised at a rate of 4 to 5 F per minute up to 340 F.

5. Cooled to 150 F, pressure released, and panels removed from the autoclave.

b. Bonding of Tip-End Masses to the Reinforcement Sheets

1. Vapor degreased

2. Etched for 10 minutes in a solution of nitric acid and a proprietary mixture containing sodium bifluoride

3. Rinsed with distilled water and dried

4. Applied FM-1000 adhesive to both, mass and reinforcement sheet

5. Placed in a platen press at 350 F for one hour

c. Bonding of Reinforcement Sheets to the Test Specimen

1. Cleaning

(a) Aluminum Test Specimens
(1) Sanded lightly and degreased
(2) Swabbed with sulfuric-dicromate solution
(3) Rinsed with distilled water and dried

(b) Stainless Steel Test Specimens

(1) Vapor degreased
(2) Swabbed with a solution of nitric acid and a proprietary mixture containing sodium fluoride
(3) Rinsed with distilled water and dried

(c) Reinforcement Sheets

(1) Removed residual adhesive from prior test by sanding
(2) Degreased
(3) Swabbed with a solution of nitric acid and a proprietary mixture containing sodium fluoride.

2. Assembly of Reinforcement Sheets to Test Specimens

(a) Applied fiberglass tape around the exposed core to prevent the expelled adhesive from flowing into the core and to assist in aligning the test panel with the reinforcement facing.

(b) Applied EC 1614 adhesive to both surfaces

(c) Cured in a platen press at 180 F for two hours

XIX INSTRUMENTATION

A schematic diagram of the circuit arrangement for the accelerometer and strain gage output signals is presented in Figure 12.

The g-loads on the specimens were sensed by three accelerometers, one mounted on each tip-end mass and one over the midspan support. The shape of the sinusoidal waves produced by the accelerometers was observed on the oscilloscopes, and frequently photographed to obtain a permanent record. These photographs were used for making comparisons, particularly congruency tests on identical specimens. A "clean" or definitive sine wave is indicative of an undisturbed specimen response while a "hashy" sine wave denotes internal disturbances in the specimen.

Readings were continuously monitored and recorded at least every ten minutes during testing. A permanent record was kept of the time, frequency, input and output g-loads, and number of accumulated cycles. This procedure was observed throughout the entire test program. Photographs of the testing equipment including the shaker are shown in Figure 13.

Prior to testing, an initial resonant frequency search was made, at a low input acceleration of about 0.5 g or less, depending upon the specimen response. The transmissibility characteristic of the specimen at resonance was subsequently checked and plotted. While maintaining resonance in the system, the input g-load was adjusted so as to produce the desired output g-load level. The same output level was maintained until final failure. Only one technician was required to conduct the complete test during the latter portion of the program. Originally, two, and often two technicians and one engineer, were necessary to observe the tests and monitor the system during testing.

One disadvantage of the dynamic test method is the need for expensive and complicated electronic instrumentation and equipment. Continuous monitoring by at least one highly skilled technician is necessary during all stages of testing. Also frequent recalibrations must be made.

A representative list of the instrumentation and equipment used in this program includes such items as:

Quantity	Item
1	Ling Power 20-KW Supply and Control Console
1	Oscillator
1	60-Minute Clock
1	RMS Ballantine Voltmeter
1	Berkeley Eput Meter (Electronic Counter)
4	Hewlett-Packard, Model 400D V.T.V.M.
1	Intercommunication System
1	Tektronix Oscilloscope, Type RM 32
1	Chadwick-Helmuth Slip Sync, Model 103A
1	Strobex 121 Lamp
1	Strobex 121R Power Supply
1	MB Electrodynamic Shaker, Model C-25H
3	Endevco Accelerometers, Model 2213
1	Endevco Amplifier Module - 6-Channel, Model 2614
2	Hewlett-Packard Oscilloscopes, Model 150A
2	Dual Trace Amplifiers, Model 152A
1	Dumont Oscillograph Recorder Camera, Type 297
1	Dumont Oscillograph Adapter
1	Emcor 6-Channel Amplifier Module
1	Transmissibility Plotter (Northrop Built)
1	Moseley Autograf Type Plotter
1	Simpson Ohm-Meter Model 260
6	Kay-Lab Amplifiers, Model 111A
-	Single-Element Budd Strain Gages
1	Consolidated Electrodynamics Recorder
1	C.E. Balance Box Carrier Signal Recorder

XX CONCLUSIONS AND RECOMMENDATIONS

The following conclusions were reached from the results obtained in this research program:

1. Fatigue properties in shear by reversed bending can be determined in sandwich constructions when using the dynamic flexural method presented in this report.

2. Reinforcement facings and concentrated tip-end masses are required in order to produce sufficiently high shear stresses in the core during long test durations of double cantilever beam specimens of relatively short span.

3. Large load amplifications can be produced at resonant frequency when the midspan support attachment is optimized with respect to adjustment and tightness.

4. The uniformity of the cell geometry and the quality of the interface bond has a very significant effect on the fatigue life of a sandwich specimen.

5. Perforations in the core were found to have no discernible effect on the fatigue life of the specimens under reversed bending loads.

6. A minimum specimen width of three inches was found to be necessary for obtaining a stable core foundation, dynamic balancing, and a minimum effect of irregular and defective core cells.

7. The effective core shear zone on each beam should contain a minimum of 100 core cells in order to obtain representative shear fatigue on the core.

8. This method is adaptable for testing at stress ratios other than R= -1 and for determining shear rigidity and viscoelastic damping.

9. This method can be used as a rapid spot-check technique for determining bond quality and face-to-core strength ratios.

If the fatigue resistance of a design which utilizes sandwich constructions is to be optimized, it is recommended that additional work be directed toward the following research studies:

1. Determine the optimum strength ratios of facings to core thicknesses and for different core densities and geometries.

2. Determine best combinations in both alloy and strength for the facings and the core material.

3. Determine contribution of cell size, cell geometry and core densities to fatigue resistance.

4. Determine trade-off point between fatigue failure and buckling instability with respect to core depth for various cell sizes and core densities.

5. Determine contribution of bonding material to fatigue resistance.

6. Determine residual fatigue life of a sandwich construction between fatigue initiation and final failure.

7. Determine effect of internal damping toward improvement of fatigue life.

8. Determine fatigue properties at cryogenic and elevated temperatures when above items are determined.

REFERENCES

1. Benson, A. S., "Dynamic Testing for Elastic Moduli of Honeycomb Cores," Northrop Corporation, Norair Division, NOR 59-384, July 1959.

2. Spector, H., "Fatigue Testing of Honeycomb Sandwich Constructions," Northrop Corporation, Norair Division, ASD TR 61-388, April 1962.

3. Apodaca, D. R., "Fatigue Testing of Sandwich Construction by Dynamic Test Method," Advanced Paper, ASME Aviation Conference, Los Angeles, March 1963.

4. Brown, Donald A., "Application of Ceramic Adhesive-Braze Alloy Combination Technique to the Bonding of Assemblies", ASD-TDR-62-631, June 1962.

5. "Honeycomb Sandwich Design Data and Test Methods," Hexcell Products, Inc., Copyright 1959.

6. ASD Data Sheets supplied with the Test Panels.

7. Roberts, W. F., and Smallen, H., "Properties of Stainless Steel Sandwich Using Low Density Honeycomb Cores," Northrop Corporation, Norair Division NOR 60-2, March 1960.

TABLES

TABLE III

DESCRIPTION OF SANDWICH TEST SPECIMENS

Specimen Type	Core Density lbs/Ft^3	Shear Strength psi (reported)	Core					Face		Specimen Dimensions, in.	Bond Core to Face
			Core Depth, in.	Cell Size, in.	Cell Geometry	Ribbon* Thick. in.	Alloy	Thick. in.	Alloy		
a	7.5	400	0.50	3/16	Square	0.0015P	PH 15-7 Mo (RH 950)	0.032	PH 15-7 Mo (RH 950)	3 x 12	Lithobraze #950
b	5.7	510	0.625	3/16	Hexagon	0.002 P	5052-H39	0.020	2024-T3	3 x 12	Adhesive FM 47
c	5.7	510	0.625	3/16	Hexagon	0.002 P	5052-H39	0.032	2024-T3	3 x 10	Adhesive FM 47
d	7.9	970	0.625	1/4	Hexagon	0.004 NP	5052-H39	0.020	2024-T3	3 x 14	Adhesive FM 61
e	5.7	510	0.625	3/16	Hexagon	0.002 P	5052-H39	0.020	2024-T3	3 x 14	Adhesive FM 47
f	10.0	1000	0.625	3/16	Hexagon	0.004 P	5052-H39	0.020	2024-T3	3 x 14	Adhesive FM 47
g	7.5	859	0.50	1/4	Square	0.002 P	17-7 PH (TH 1050)	0.050	17-7 PH (TH 1050)	3 x 14	Braze**

* P = perforated

* NP = non-perforated

** GFE - furnished Solar panels, No. 1C

Note: Valid fatigue test data was developed for specimens of Types d, e, and g only. S-N fatigue curves for these three materials are presented in Figure 8, 9, & 10.

TABLE IV

FATIGUE TEST DATA FOR VARIOUS SANDWICH CONSTRUCTION AND CONFIGURATIONS - FEASIBILITY STUDIES

Specimen No.	Test Config-uration	Specimen Type	Resonant Frequency cps	Wt. of Mass/End lbs.	Max. Transmitted Force				Cycles 10^3	Total Cycles 10^3	Remarks
					Beam No. 1		Beam No. 2				
					g-load	shear stress, psi	g-load	shear stress, psi			
1	A	a	258	0.61	120-262	44.4-96.9	131-262	48.5-96.9		4,990.0	crushing of core between end-masses
2	A	b	224	0.61	105-119	33.1-37.5	122-138	38.4-43.5		3,090.0	both facings failed in fatigue
3	A	b	200	0.61	190	59.9	180	56.7		390.0	facing failed in fatigue
4	B	c	276	1.1	125-190	69.8-106	125-175	69.8-97.7		950.0	facing failed in fatigue
5	B	c	275	1.1	150	83.7	153	85.4		810.0	facing failed in fatigue
6	C	b	227	1.1	-	-	-	-		14.0	bond failure between insert halves
7	D	b	209	1.0	50-125	25-64	85	43		69.0	discontinued due to Hg leakage
8	D	a	292	1.0	25-90	16-59	25	16		5,310.0	discontinued due to Hg leakage
9	E	d	228	1.1	150-250	85.2-142	155-253	88.0-144		600.0	facing failed in fatigue
10	E	d	228	1.1	250	142	-	-		66.0	reinforcement facing failed in fatigue
11	F	d	208	2.9	80-190	285 MAX	82-190	285 MAX		12.0	facing-to-core glueline failure
12	F	d	210	2.9	100-125*	150-188	105-123*	158-185		1,470.0	core fatigue failure
13	F	d	211	2.9	120	169	121	171		229.0	reinforcement facing bond failure
14	F	d	207	2.9	120-125*	169-176	125-135	176-190		64.0	core fatigue failure
15	F	e	204	3.02	100	140	100	140		10.0	overload shear failure
16	F	e	194	3.02	50	70	50	70	116.3		**
					100	140	100	140	10.0	126.3	overload shear failure
17	F	e	196	3.02	50	70	50	70	354.2		**
					60*	84	60	84	135.5	489.7	core fatigue failure
18	F	e	180	3.02	50*	70	50	70		213.4	core fatigue failure
19	F	e	198	3.02	40	56	40	56	5,000.0		**
					45	63	45	63	1,000.0		**
					50	70	50	70	1,000.0		**
					55	77	55	77	1,420.0		**
					60	84	60	84	1,019.0		**
					65	91	65*	91	44.0	9,483.0	core fatigue failure
20	F	e	185	3.02	89*	125	90	126		234.8	core fatigue failure
21	F	e	194	3.02	84	118	85	119	10,000.0		**
					89	125	90	126	1,000.0		**
					99	139	100	140	500.0		**
					109	153	110	154	500.0		**
					120	168	120	162	250.0		**
					130*	182	130	182	32.6	12,282.0	core fatigue failure
22	F	e	192	3.02	130	182	130	182	2.0		transmissibility check
					120	168	120	168	361.8	363.8	core fatigue failure
23	F	f	191	3.02	130	182	130	182	2.0		transmissibility check
					120	168	115	168	94.0	96.0	core fatigue failure
24	F	f	190	3.02	130	182	130	182	2.0		transmissibility check
					108	151	110	154	222.9	224.9	core fatigue failure

* Denotes beam containing the greatest degree of damage.

** Same specimen retested and presented in the following line.

TABLE V

TEST RESULTS USED FOR FATIGUE CURVE DEVELOPMENT -
TYPE D SPECIMENS, ADHESIVE-BONDED ALUMINUM 5052-H39,
CORE DENSITY - 7.9 PCF

Specimen No.	Resonant Frequency cps	Wt. of Mass/End lbs	Max. Transmitted Force				Cycles 10^3	Total Cycles 10^3	Remarks
			Beam No. 1		Beam No. 2				
			g-load	shear stress, psi	g-load	shear stress, psi			
1	198	3.0	100	140	97	136	1,246.7		retested at higher load
			150	210	153	214	2,471.5	3,818.2	destroyed during inspection
2	197	3.0	125	175	125	175	11,000.0**		retested at higher load
			150	210	150	210	817.0	11,817.0	facing failed in fatigue
3	196	3.0	165	231	165	231		631.0	bond failure between facing & reinforcement
4	194	3.0	170*	238	165	231		226.0**	core fatigue failure
5	195	3.0	160	224	155*	217		767.0**	core fatigue failure
6	195	3.0	155	217	152	213		514.8	bond failure between facing & reinforcement
7	196	3.0	150	210	152	213		173.9	bond failure between facing & reinforcement
8	194	3.0	150	210	148	207	381.0		bond failure as above, repaired, test resumed
	188	3.0	150	210	147	206	47.0		bond failure as above, repaired, test resumed
	175	3.0	150	210	145	203	2.0	430.5	core fatigue failure
9	196	3.0	145*	203	140	196	428.4		bond failure as above, repaired, test resumed
10	195	3.15	180	263	185*	270	7.1	435.5	destroyed during inspection
11	195	3.16	168*	245	176	256		10.0	(specimens 10 thru 15 failed pre-
12	192	3.19	120	178	120*	178		7.8	maturely due to stress concentrations
13	208	3.19	130*	192	140	207		7.6	within the core resulting from irreg-
14	187	3.15	185	270	185*	270		51.0	ular core cell geometry (see text)
15	201	3.19	150	220	150*	220		2.0	
								12.0	

* Denotes beam containing the greatest degree of fatigue damage.
** Only specimens from which results were plotted as valid.

TABLE VI

TEST RESULTS USED FOR FATIGUE CURVE DEVELOPMENT, TYPE E SPECIMENS ADHESIVE-BONDED ALUMINUM 5052-H39, CORE DENSITY - 5.7 PCF

Specimen No.	Resonant Frequency cps	Wt. of Mass/End lbs.	Max. Transmitted Force				Total Cycles 10^3	Remarks
			Beam No. 1		Beam No. 2			
			g-load	shear stress, psi	g-load	shear stress, psi		
1	194	3.19	60	89	59	87	10,000.0	test discontinued
2	193	3.19	135*	200	130	192	147.0	core fatigue failure
3	193	3.19	180	118	78*	115	4,622.0	core fatigue failure
4	197	3.19	125*	185	123	182	119.3	core fatigue failure
5	187	3.02	115*	161	113	158	564.3	core fatigue failure
6	193	3.19	110*	163	107	158	397.7	core fatigue failure
7	183	3.15	103*	150	105	153	173.5	core fatigue failure
8	196	3.19	100	148	95*	141	1,146.0	core fatigue failure
9	190	3.19	95*	141	95	141	454.0	core fatigue failure
10	192	3.19	130	192	126*	186	368.0	core fatigue failure
11	190	3.16	150	219	142*	207	21.0	core fatigue failure
12	185	3.15	80	117	80*	117	2,807.0	core fatigue failure

* Denotes beam containing the greatest degree of fatigue damage.

TABLE VII

TEST RESULTS USED FOR FATIGUE CURVE DEVELOPMENT - TYPE G SPECIMENS SOLAR-BRAZED 17-7 PH (TH 1050) STAINLESS, CORE DENSITY - 7.5 PCF

Specimen No.	Resonant Frequency cps	Wt. of Mass/end lbs.	Max. Transmitted Force				Total Cycles	Remarks
			Beam No. 1		Beam No. 2			
			g-load	shear stress, psi	g-load	shear stress, psi		
1	198	3.19	110	190	107	185	203.5	transmissibility check
2	195	3.19	90	156	87*	151	613.4	core fatigue failure
3	200	3.19	80*	138	78*	135	5,177.8	core fatigue failure
4	197	3.19	90*	156	87	151	1,841.8	core fatigue failure
5	191	3.14	100	171	97*	166	484.0	core fatigue failure
6	191	3.16	115	198	113*	194	336.0	core fatigue failure
7	187	3.15	75	128	70*	120	8,648.0	core fatigue failure
8	193	3.19	100*	173	100	173	481.0	core fatigue failure
9	189	3.02	140*	230	-	-	64.0	core fatigue failure
10	197	3.19	80	138	76	131	10,000.0	test discontinued
11	197	3.19	115*	199	111	192	787.0	core fatigue failure
12	196	3.19	120	208	110*	190	654.0	core fatigue failure
13	188	3.02	130*	213	130	213	180.0	core fatigue failure

* Denotes beam containing the greatest degree of fatigue failure.

ILLUSTRATIONS

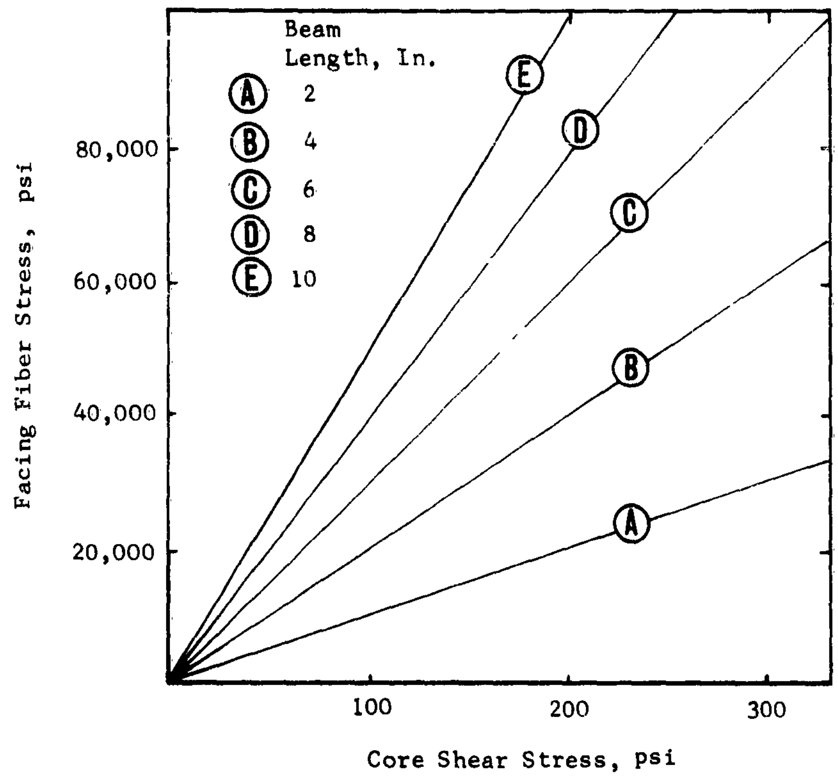

(a) Aluminum Specimen Types b, d, and e with 0.020" facings

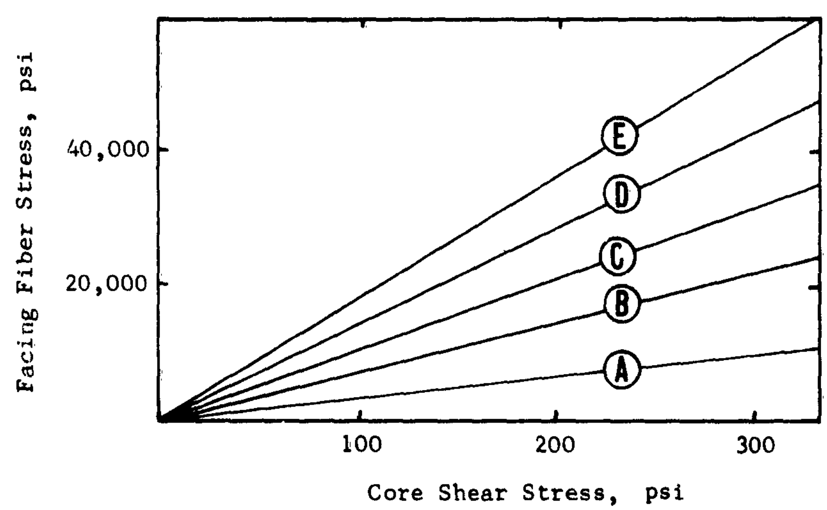

(b) Stainless Steel Specimen Type g with 0.050 inch facings

FIGURE 1 A GENERAL PARAMETER RELATING THE FACING FIBER STRESS TO THE CORE SHEAR STRESS PRODUCED BY BENDING OF A 3" WIDE CANTILEVER BEAM

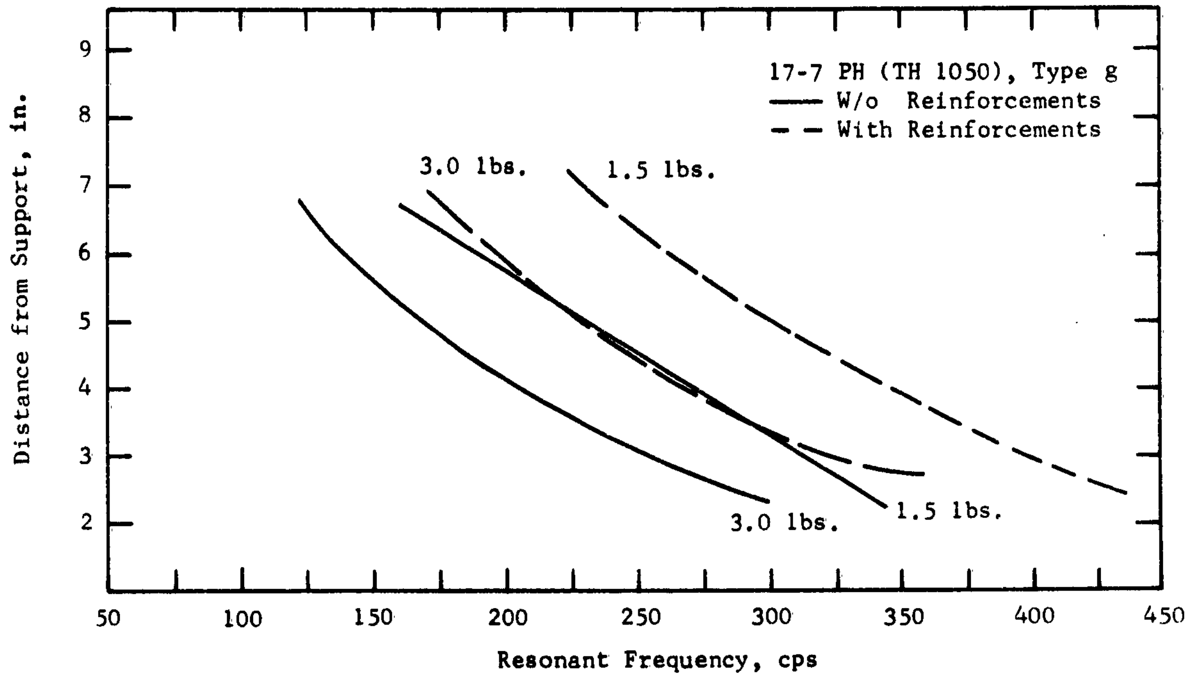

(a) Stainless Steel Sandwich Specimen

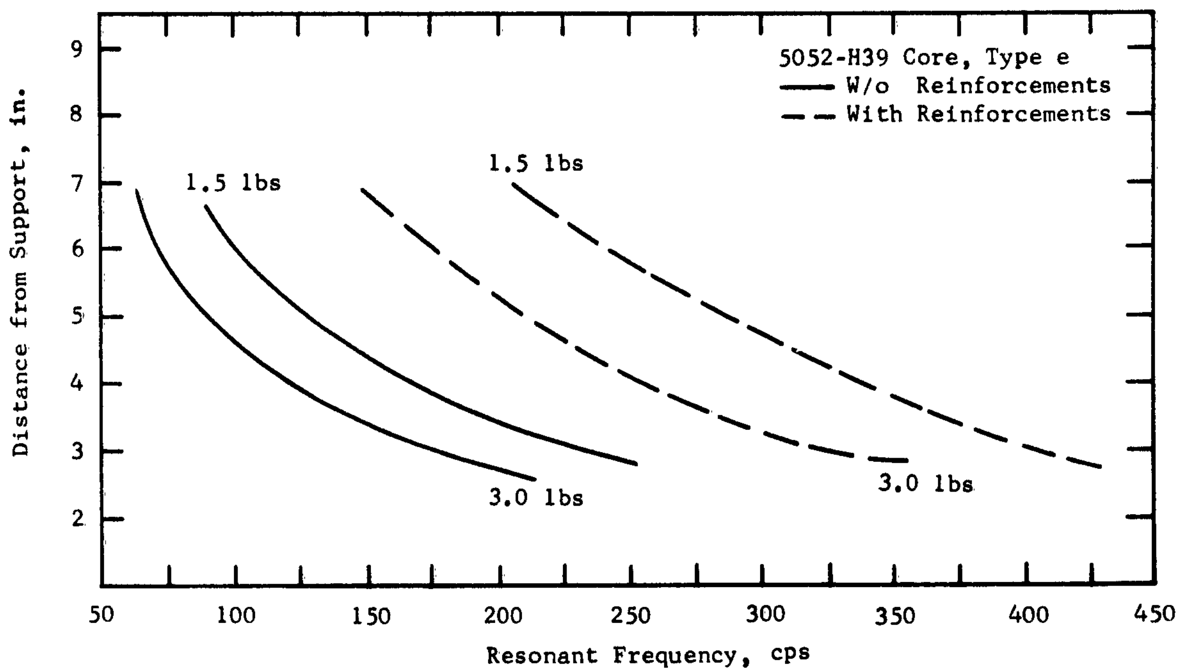

(b) Aluminum Alloy Sandwich Specimen

FIGURE 2 EFFECT OF WEIGHT AND LOCATION OF MASSES, WITH AND WITHOUT REINFORCEMENT FACINGS, ON THE RESONANT FREQUENCY

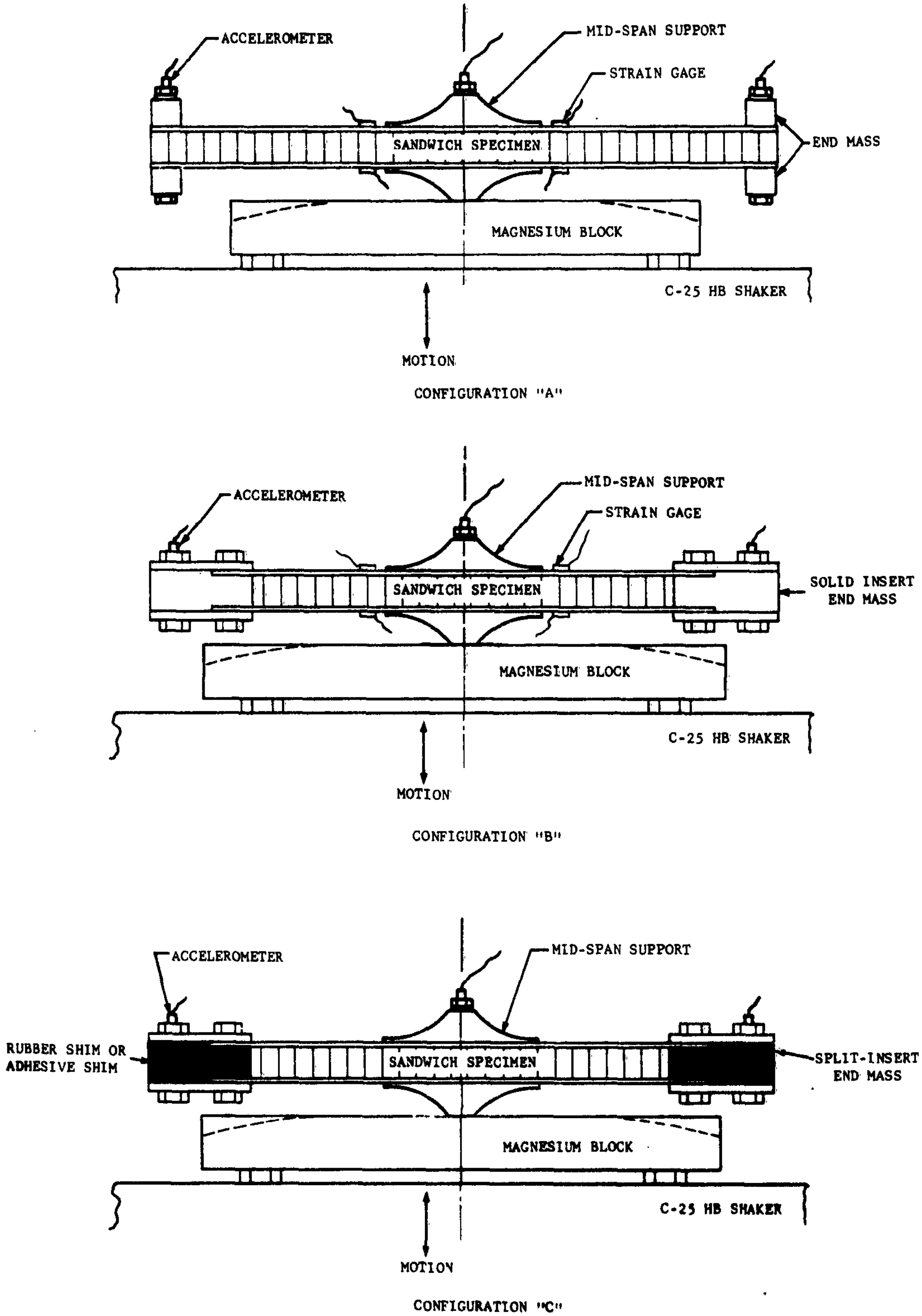

FIGURE 3 SCHEMATIC OF SPECIMEN CONFIGURATIONS STUDIED FOR TESTING TO PRODUCE FATIGUE IN SHEAR BY BENDING

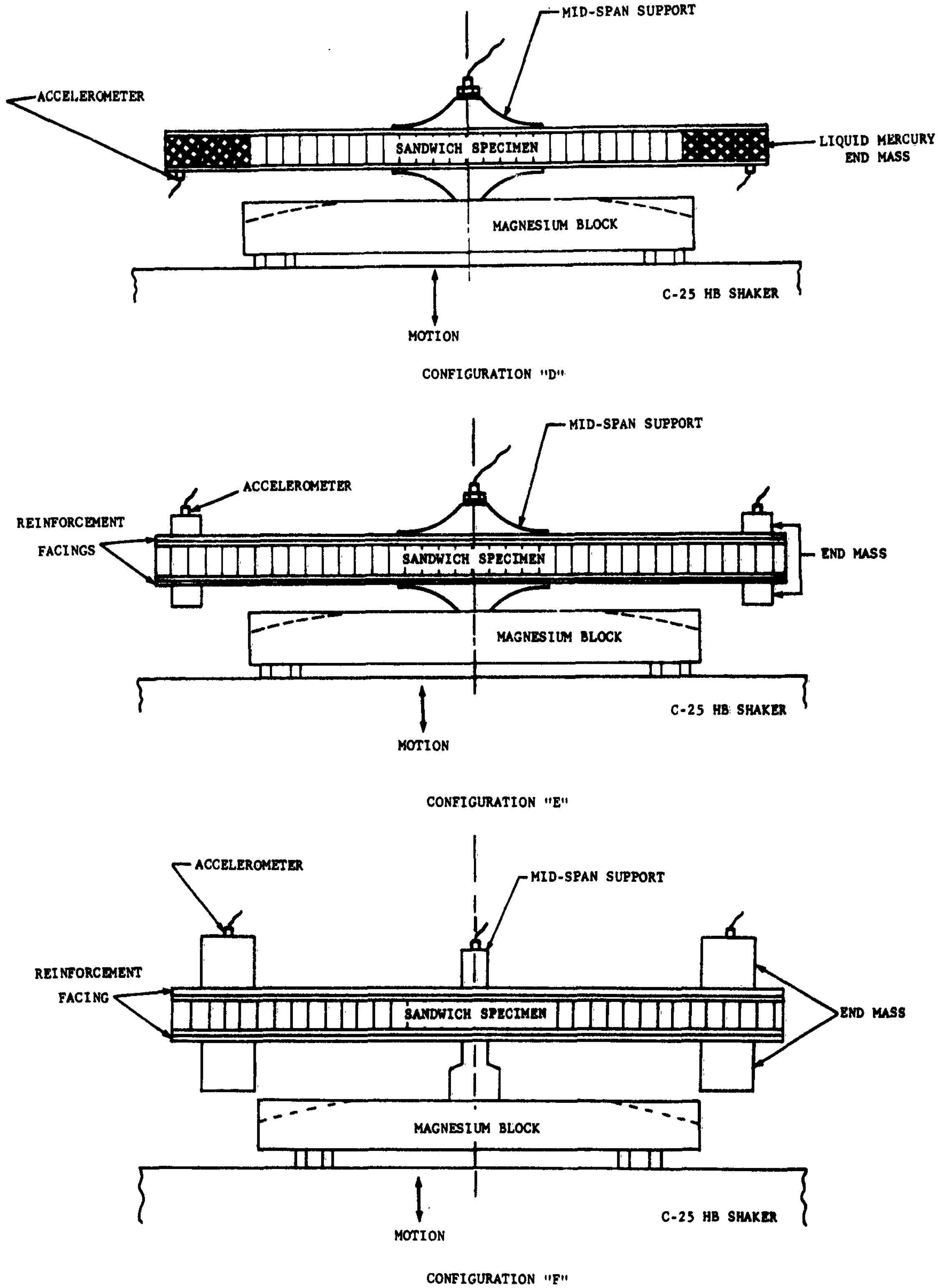

FIGURE 4 SCHEMATIC OF SPECIMEN CONFIGURATIONS STUDIED FOR TESTING TO PRODUCE FATIGUE IN SHEAR BY BENDING

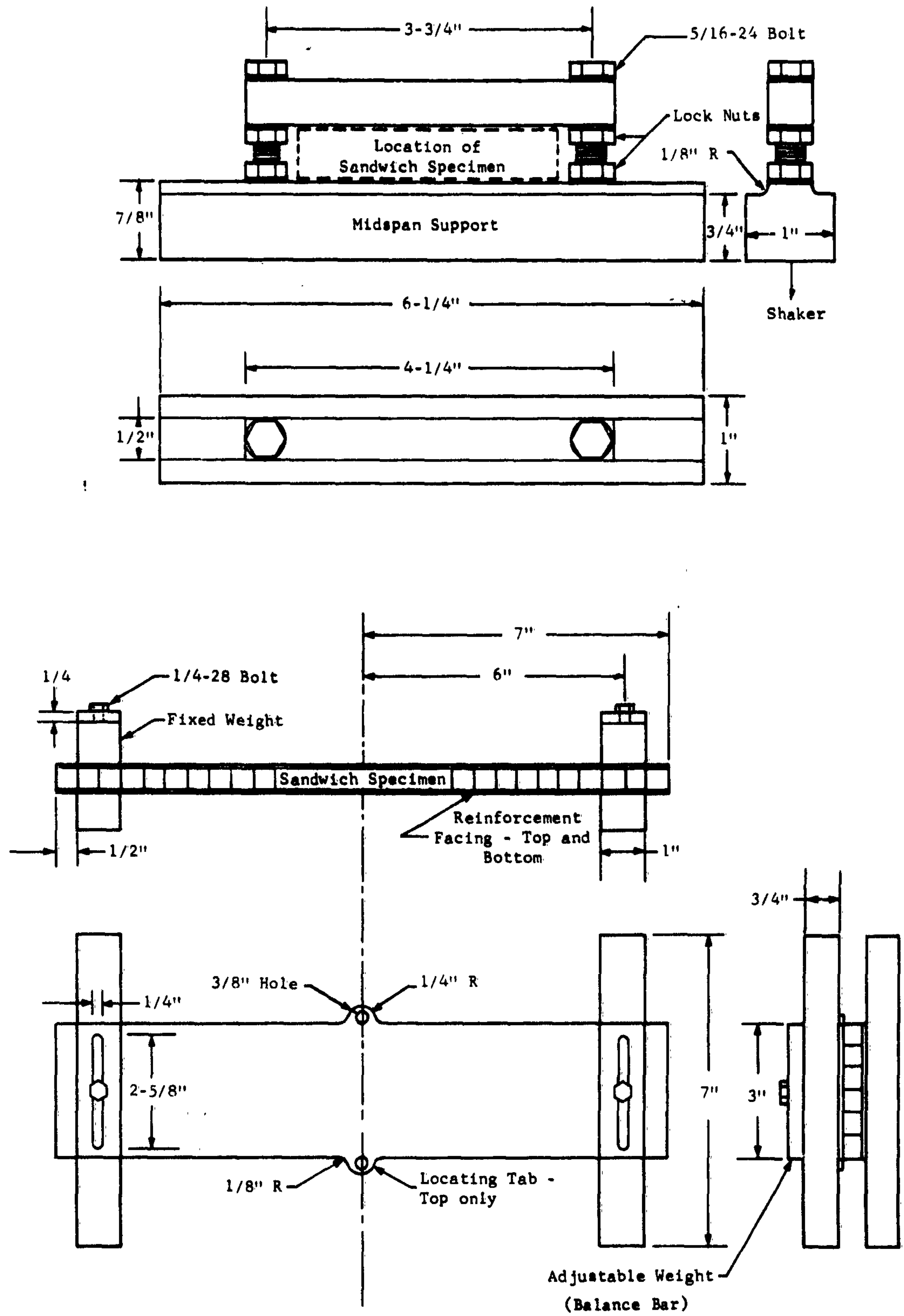

FIGURE 5 DETAIL DRAWING OF REINFORCEMENT FACING WITH TIP END WEIGHTS

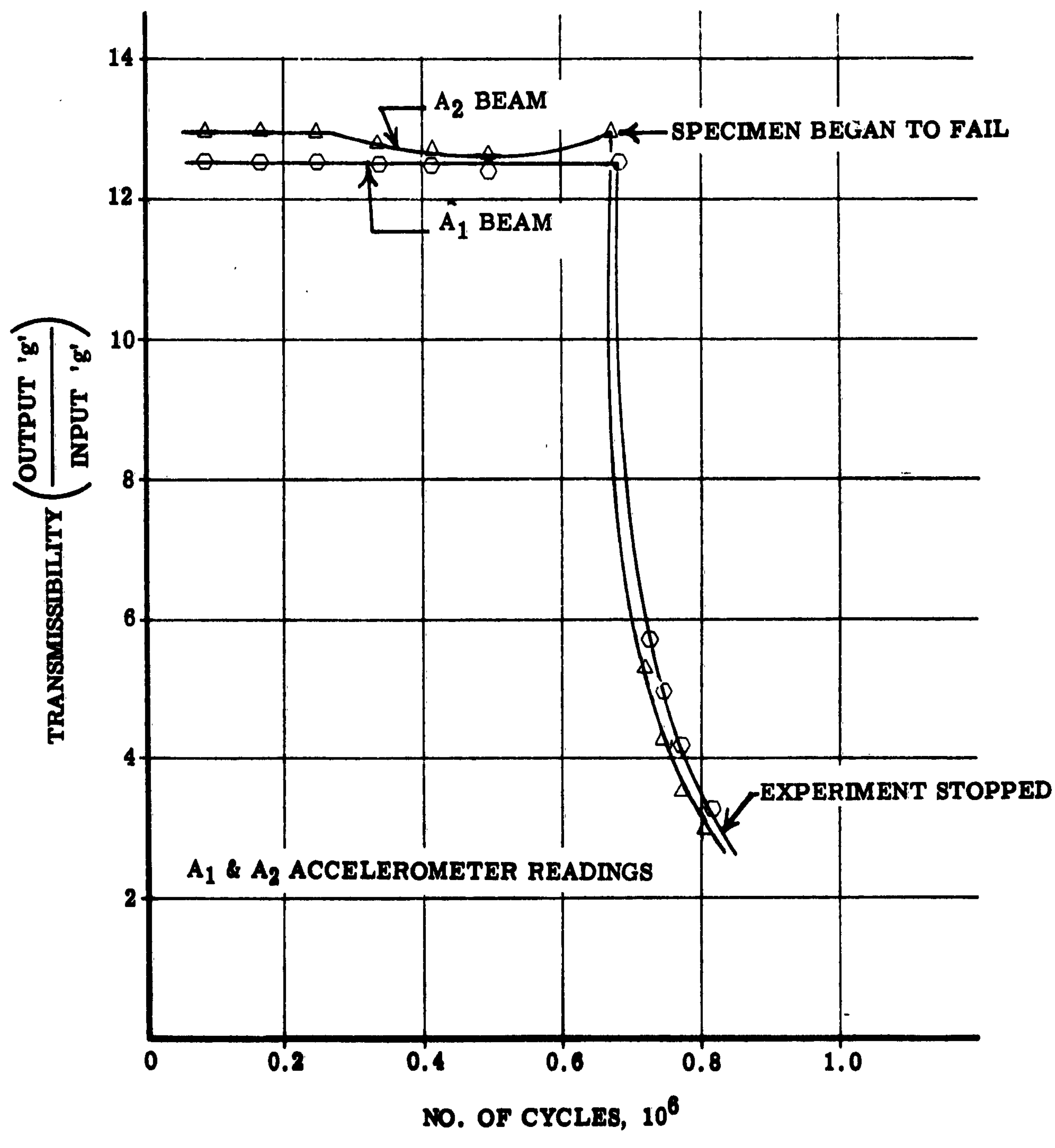

FIGURE 6 TRANSMISSIBILITY RESPONSE FROM TEST INITIATION TO FINAL FAILURE FOR SPECIMEN 5 (FEASIBILITY STUDIES)

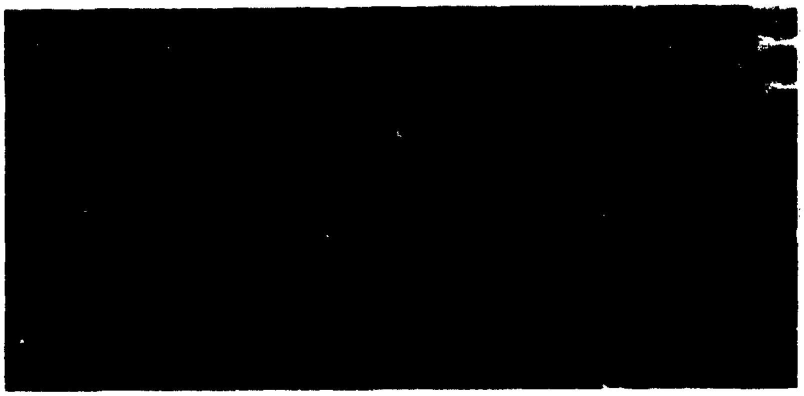

(a) Aluminum Type d Specimen

(b) Aluminum Type e Specimen

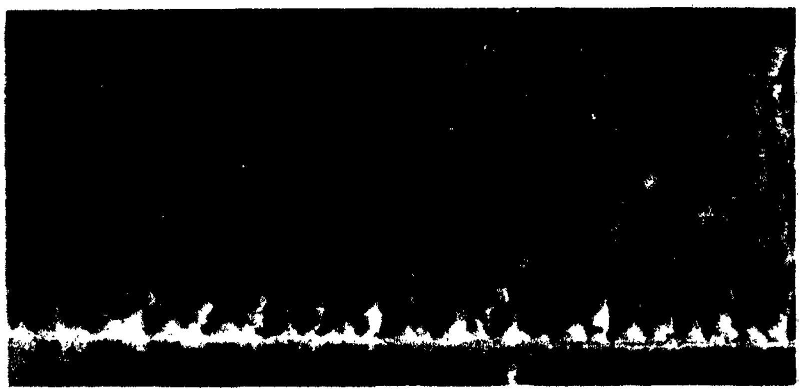

(c) Stainless Steel Type g Specimen

FIGURE 7 TYPICAL CORE FATIGUE FAILURES OF SANDWICH TEST SPECIMENS

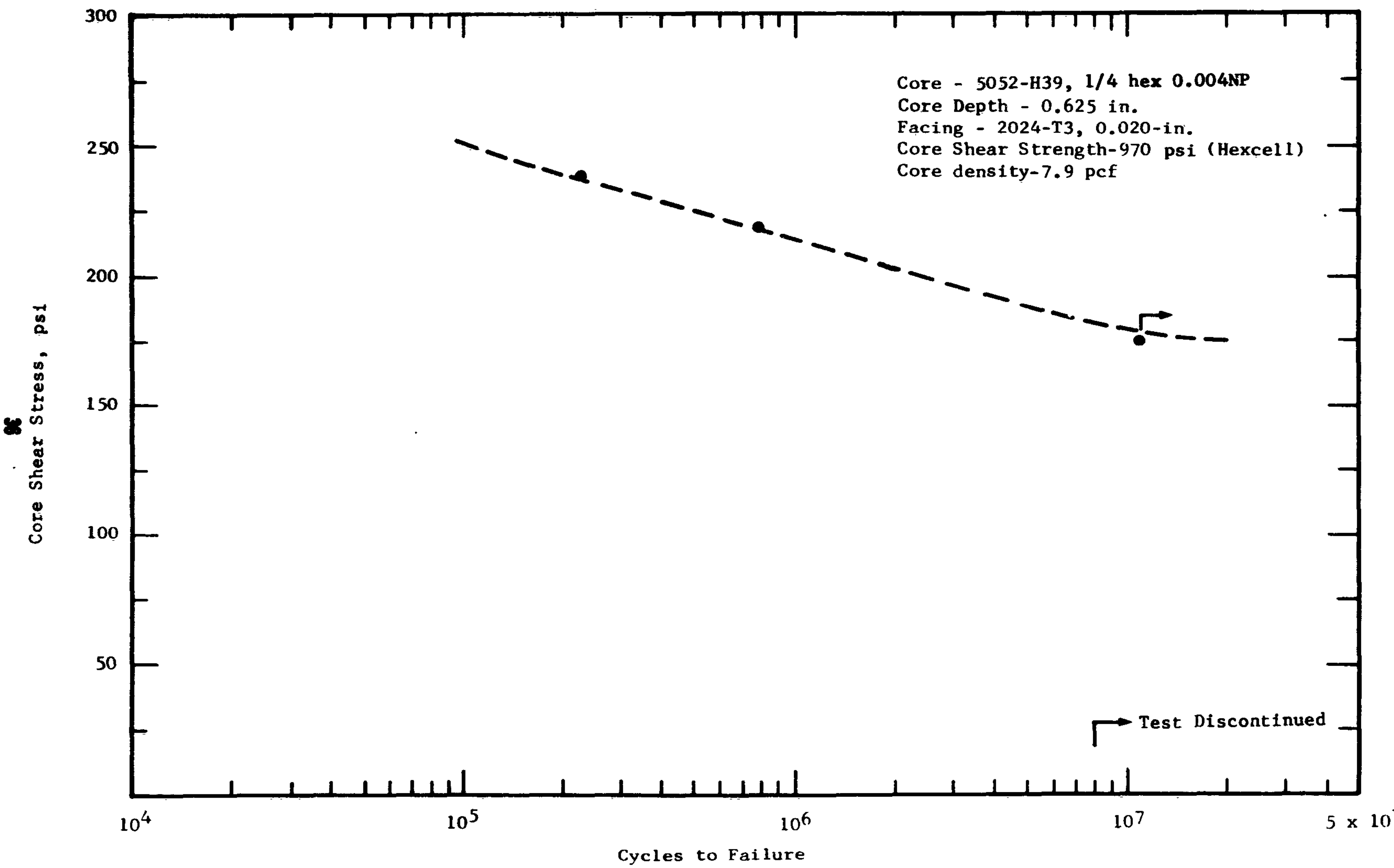

FIGURE 8 FATIGUE PROPERTIES IN SHEAR OF ADHESIVE-BONDED 5052-H39 ALUMINUM ALLOY TYPE D SANDWICH SPECIMENS, R = -1

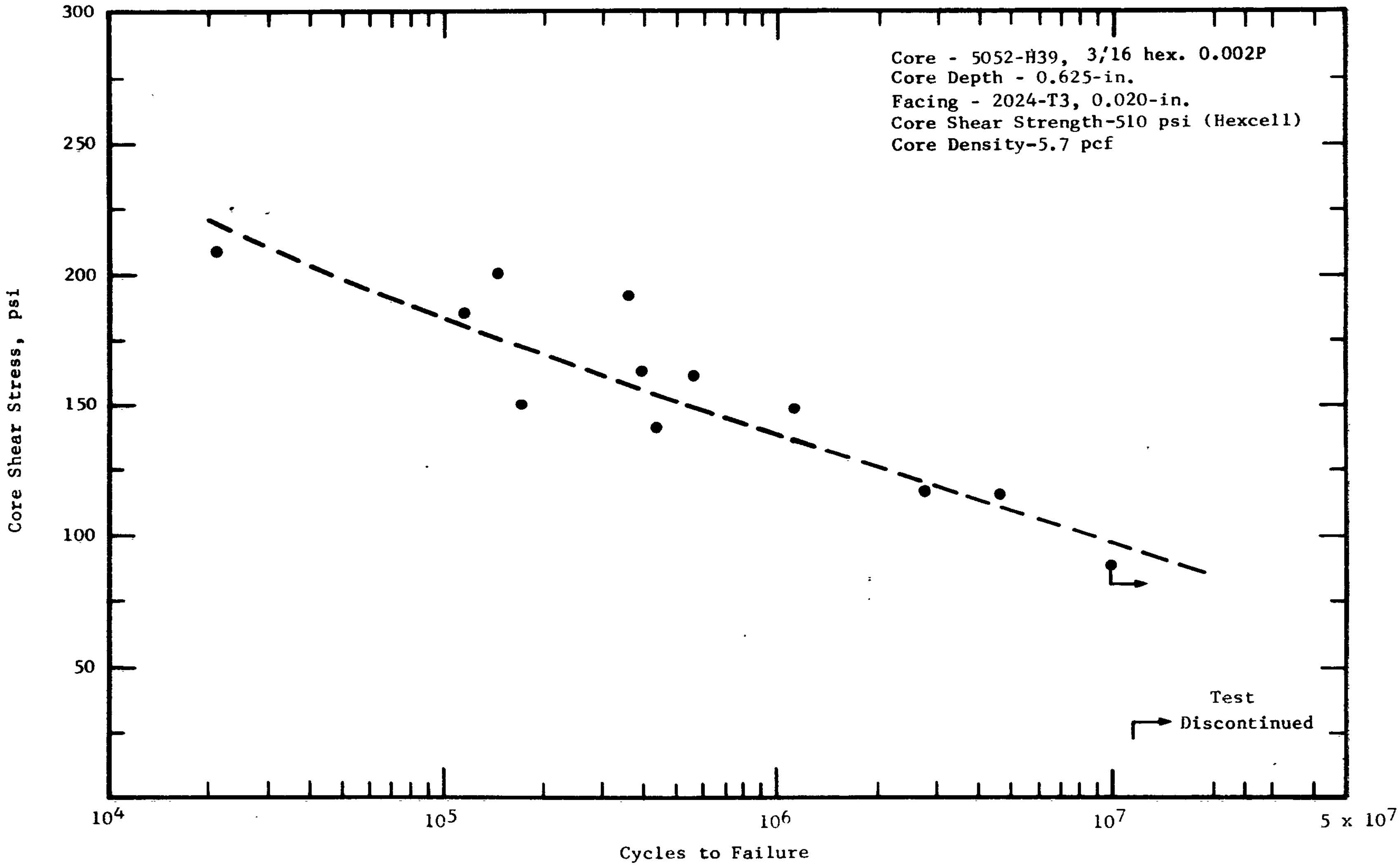

FIGURE 9 FATIGUE PROPERTIES IN SHEAR OF ADHESIVE-BONDED 5052-H39 ALUMINUM ALLOY TYPE E SANDWICH SPECIMENS, R = -1

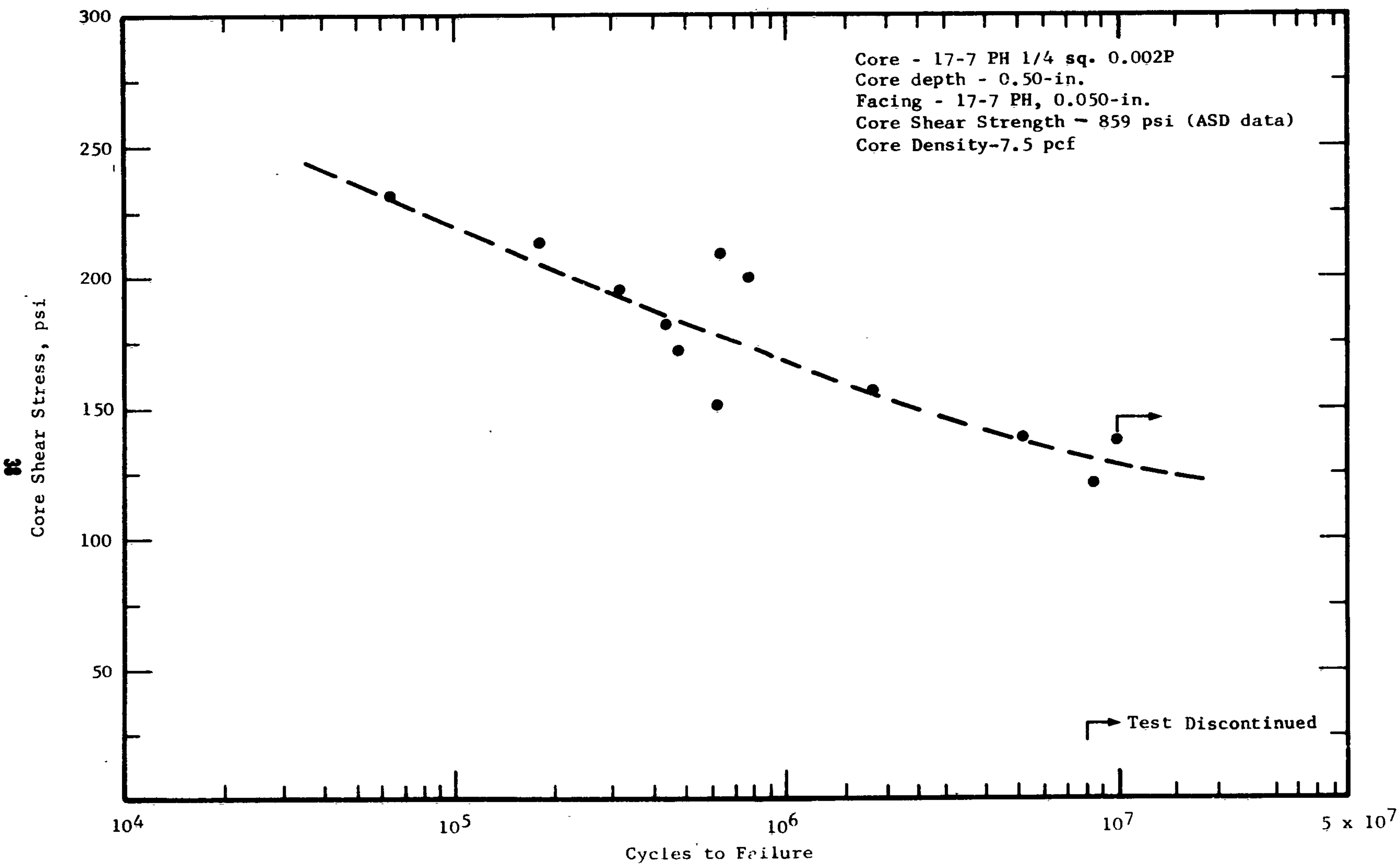

FIGURE 10 FATIGUE PROPERTIES IN SHEAR OF BRAZED 17-7 PH (TH 1050) STAINLESS STEEL TYPE G SANDWICH SPECIMENS, R = -1

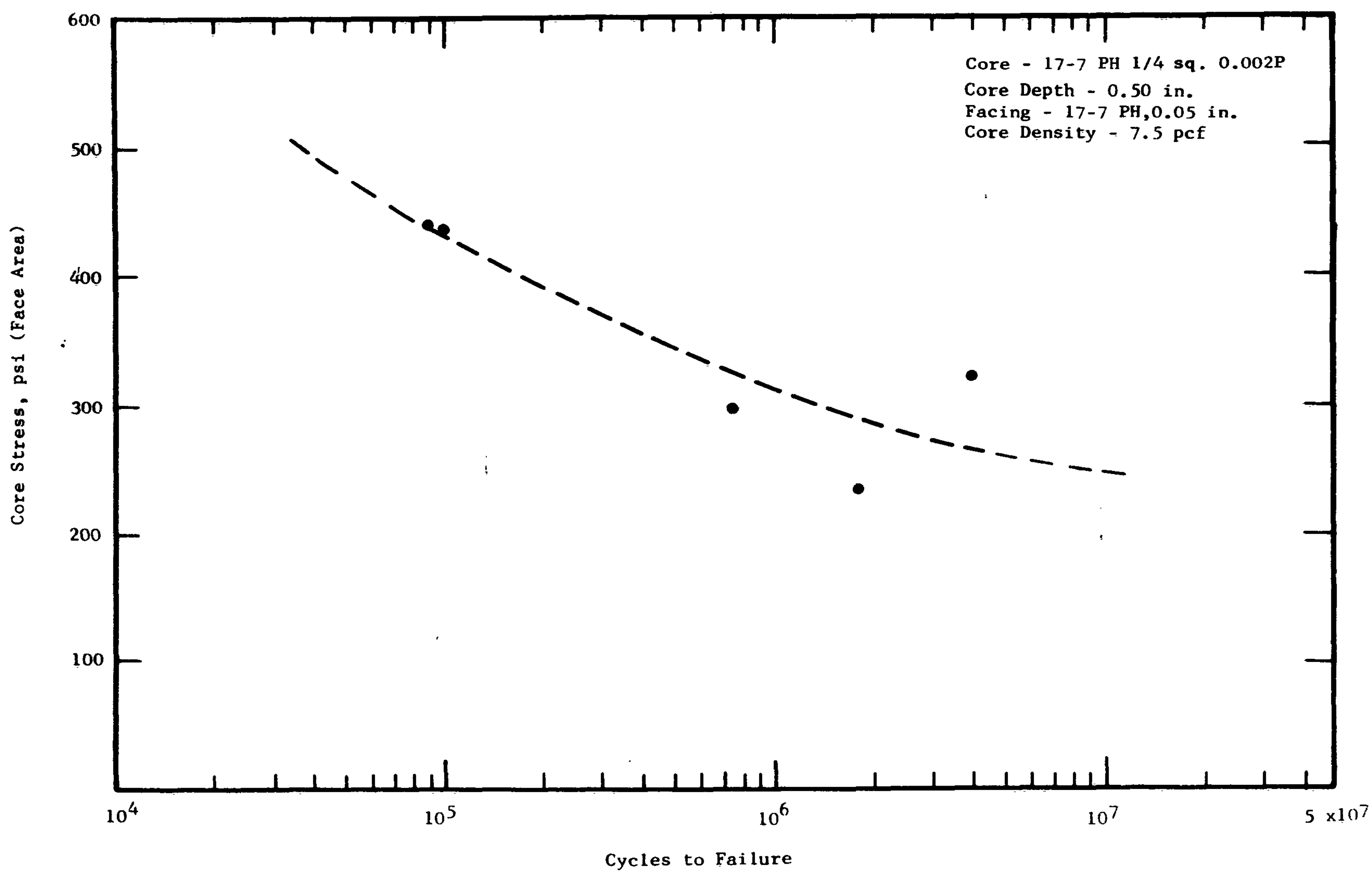

FIGURE 11 FATIGUE PROPERTIES IN TENSION-COMPRESSION OF BRAZED 17-7 PH (TH 1050) STAINLESS STEEL TYPE G SANDWICH SPECIMENS, R = -1. (REFERENCE 2)

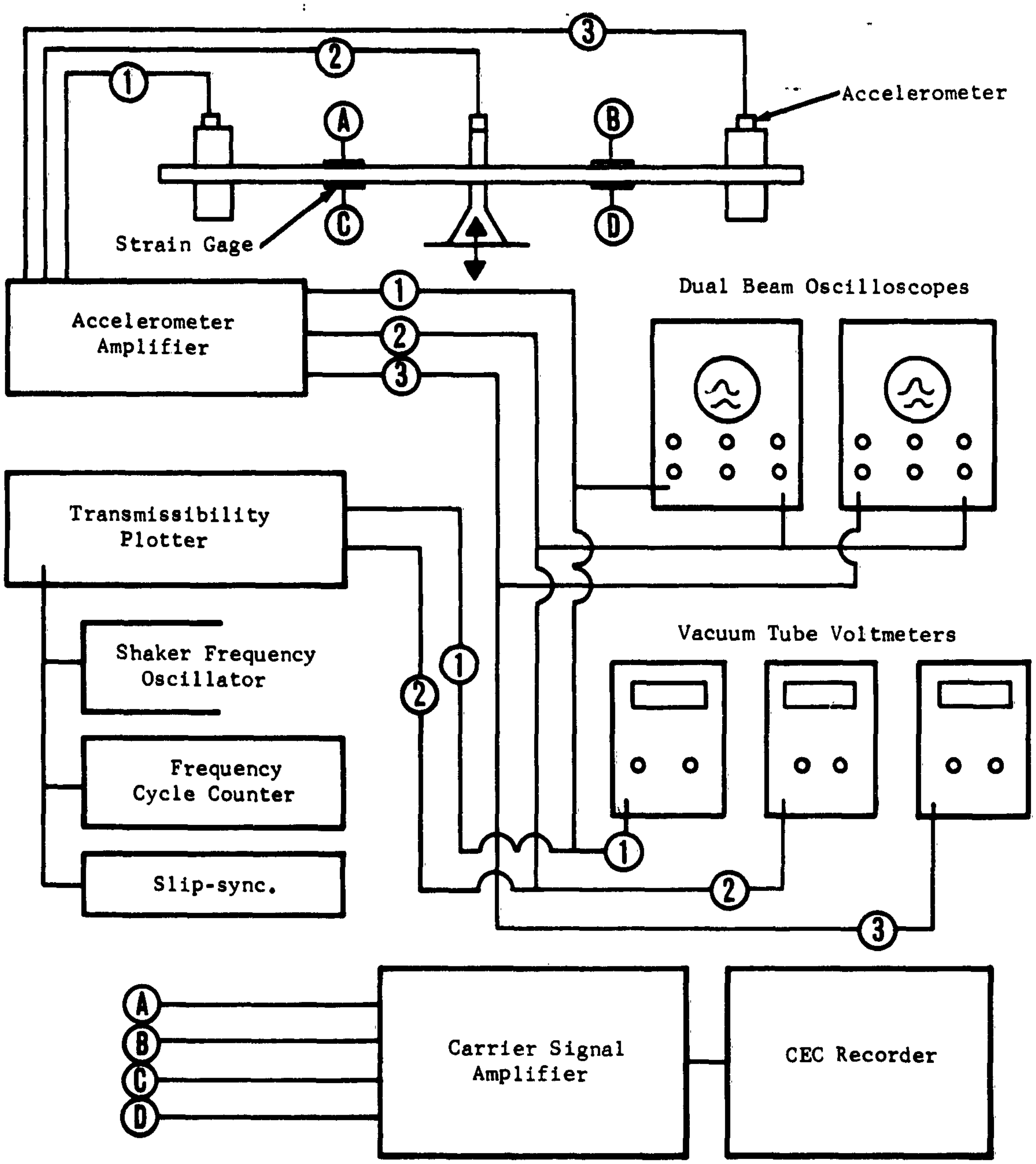

FIGURE 12 INSTRUMENTATION ARRANGEMENT FOR ACCELEROMETERS AND STRAIN GAGES USED DURING FATIGUE TESTING

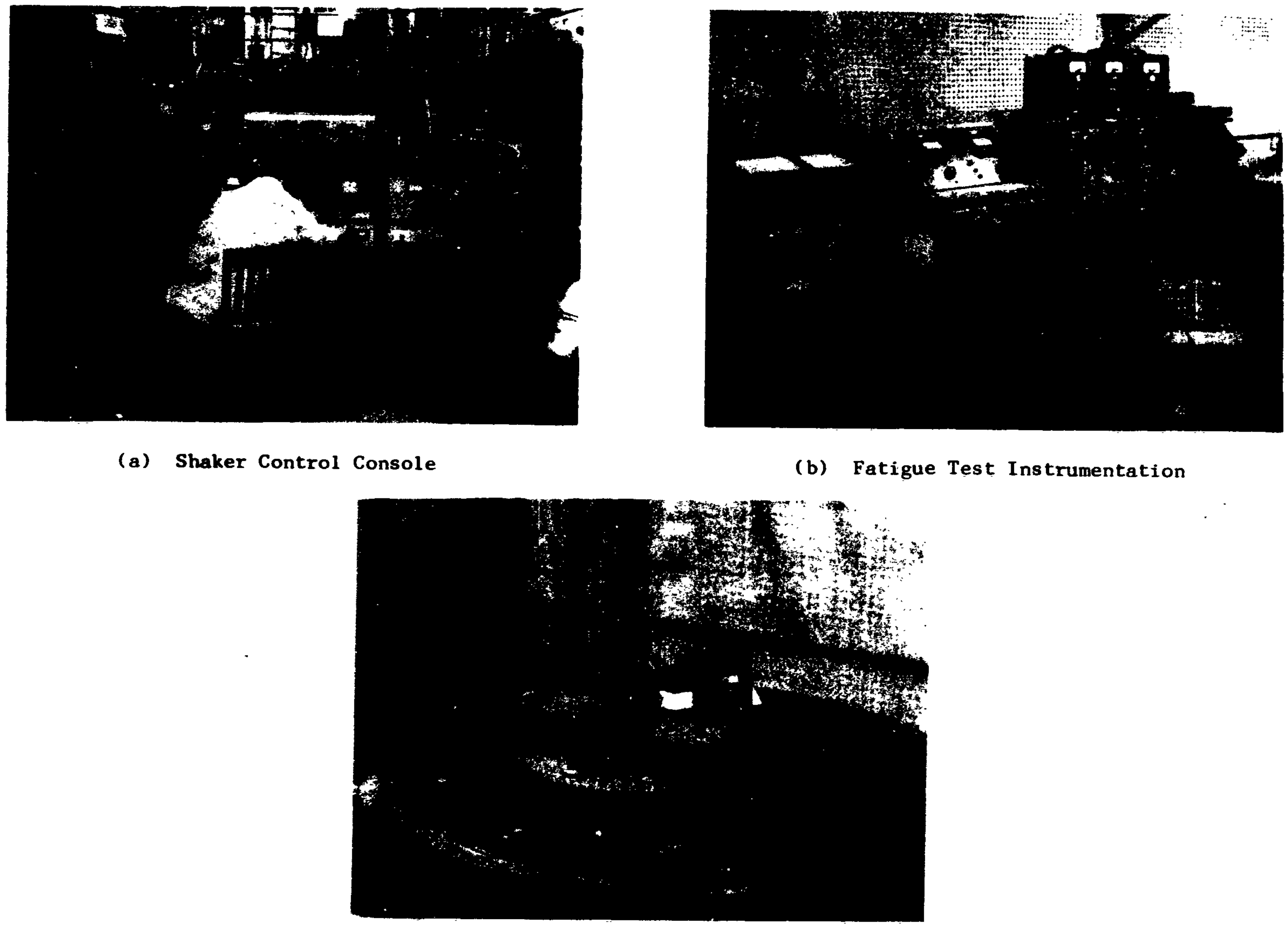

(a) Shaker Control Console

(b) Fatigue Test Instrumentation

(c) Configuration F Mounted on Shaker

FIGURE 13 EQUIPMENT USED FOR CONDUCTING FATIGUE TESTS IN SHEAR ON SANDWICH SPECIMENS

APPENDIX A

NOTATIONS FOR ANALYTICAL EVALUATIONS

APPENDIX A

NOTATIONS FOR ANALYTICAL EVALUATIONS

Listed below are the symbols used in this appendix.

A = Area, in^2
b = Width of the specimen, in
E = Modulus of elasticity, lb/in^2
E_s = Modulus of elasticity (specimen facings) lbs/in^2
E_r = Modulus of elasticity (reinforcement facings) lbs/in^2
G = Shear Modulus lbs/in^2
g = Direct accelerometer reading - the ratio of the acceleration of the specimen mass to the acceleration due to gravity
I = Moment of inertia of an area, in^4
k = Constant
K = Spring constant, lbs/in
P = Load, lbs
M = Bending moment, in-lb
W = Weight of end-masses, lbs
L = Length of effective span, in
ω = Natural frequency, rad/sec
Q = First moment of area, in^3
t = Total thickness of the specimen, in
t_c = Thickness of the core, in
t_f - Thickness of panel facing , in
t_r = Thickness of the reinforcement facing, in
V = Shearing force, lbs
τ = Shear stress, lbs/in^2
σ = Stress, lbs/in^2
δ_b = Bending deflection, in
δ_s = Shear deflection, in

The following formulae were used for obtaining the relationships of the specimen configurations, and for calculating test results.

When determining the shear stresses within the core, the sandwich specimen is compared to an I-beam, i.e., the facings correspond to the flanges and the core to the webs, thus

1) Core Shear Stress $\tau = \dfrac{QV}{bI}$ where $V = Wg$ (1)

2) Facing Fiber Stress $\sigma = \dfrac{Mt}{2I}$ (2)

3) The following relationships were used to develop the moment of the area and the moment of inertia of the composite with and without the reinforcement facings

$$I = I_o^o + Ad^2$$

without the reinforcement facing

$$I = 2t_f b \left(\frac{t_c}{2} + \frac{t_f}{2}\right)^2 \qquad (3)$$

$$Q = t_f b \left(\frac{t_c}{2} + \frac{t_f}{2}\right) \tag{4}$$

with the reinforcement facing - developed by the transformed section method where the steel reinforcement sheet is replaced by an equivalent sheet of aluminum $\left(\frac{E_r}{E_s} \; b \; t_r\right)$

$$I = 2 \, t_r \, b \, \frac{E_r}{E_s} \left(\frac{t_c}{2} + t_f + \frac{t_r}{2}\right)^2 + 2 \, t_f \, b \left(\frac{t_c}{2} + \frac{t_f}{2}\right)^2 \tag{5}$$

$$Q = t_r \, b \, \frac{E_r}{E_s} \left(\frac{t_c}{2} + t_f + \frac{t_r}{2}\right) + t_f \, b \left(\frac{t_c}{2} + \frac{t_f}{2}\right) \tag{6}$$

4) In determining the fiber stress developed in the aluminum sandwich facing and the steel reinforcement facing, the following relations were applied.

Aluminum facing

$$\sigma_{max} \cong \frac{M}{b \, t_c \left(\frac{E_r}{E_s} \, t_r + t_f\right)} \tag{7}$$

Steel reinforcement facing

$$\sigma_{max} \cong \frac{M}{b \, t_c \left(t_r + \frac{E_s}{E_r} \, t_f\right)} \tag{8}$$

5) For a cantilever sandwich beam whose distributed mass is small compared to the end mass, the end mass constitutes a single degree of freedom whose natural frequency is given by

$$\omega^2 = \frac{K}{m} \tag{9}$$

where a cantilever beam with a point load applied at the free end

$$K = \frac{1}{\delta_b} + \frac{1}{\delta_s} \tag{10}$$

or

$$K = \frac{1}{\frac{L^3}{3 \, EI} + \frac{L}{Gk}} \tag{11}$$

6) The effective concentrated weight (W_e) of the reinforcement facings was determined from the change in resonant frequency (Table I) for two different mass weights (W_1 and W_2) in a specimen with and without reinforcement facings.

$$W_e = \underbrace{\left[\frac{\omega_2^2 W_2 - \omega_1^2 W_1}{\omega_1^2 - \omega_2^2}\right]}_{\text{with reinforcement facings}} - \underbrace{\left[\frac{\omega_4^2 W_2 - \omega_3^2 W_1}{\omega_3^2 - \omega_4^2}\right]}_{\text{without reinforcement facings}} \qquad (12)$$

Aeronautical Systems Division, Dir/Materials and Processes, Applications Lab, Wright-Patterson AFB, Ohio.
Rpt Nr ASD-TR-61-338, Part II. FATIGUE IN SHEAR BY BENDING OF STRUCTURAL SANDWICH CONSTRUCTIONS. Final report, Mar 63, 45p. incl illus., tables, 7 refs.
Unclassified Report

The Dynamic Test Method has been successfully applied for obtaining core fatigue in shear by reversed bending of a double cantilever beam sandwich specimen containing heavy tip-end masses. The testing approach consists of applying forced vibrations at resonant frequency with an electromagnetic shaker for each stress level desired.

1. Sandwich construction
2. Fatigue testing
3. Test method
I. AFSC Project 7381,Task 738103
II. Contract AF 33 (657)-7309
III. Northrop Corp. Norair Div. Hawthorne, Calif.
IV. D. R. Apodaca
J. L. Preston
V. Secondary Rpt No. NOR 63-25
VI. Not aval fr OTS
VII. In ASTIA collection

Aeronautical Systems Division, Dir/Materials and Processes, Applications Lab, Wright-Patterson AFB, Ohio
Rpt Nr ASD-TR-61-338, Part II. FATIGUE IN SHEAR BY BENDING OF STRUCTURAL SANDWICH CONSTRUCTIONS. Final report, Mar 63, 45p. incl illus., tables, 7 refs.
Unclassified Report

The Dynamic Test Method has been successfully applied for obtaining core fatigue in shear by reversed bending of a double cantilever beam sandwich specimen containing heavy tip-end masses. The testing approach consists of applying forced vibrations at resonant frequency with an electromagnetic shaker for each stress level desired.

1. Sandwich construction
2. Fatigue testing
3. Test method
I. AFSC Project 7381, Task 738103
II. Contract AF 33 (657)-7309
III. Northrop Corp. Norair Div. Hawthorne, Calif.
IV. D. R. Apodaca
J. L. Preston
V. Secondary Rpt No. NOR 63-25
VI. Not aval fr OTS
VII. In ASTIA collection

Aeronautical Systems Division, Dir/Materials and Processes, Applications Lab, Wright-Patterson AFB, Ohio.
Rpt Nr ASD-TR-61-338, Part II. FATIGUE IN SHEAR BY BENDING OF STRUCTURAL SANDWICH CONSTRUCTIONS. Final report, Mar 63, 45p. incl illus., tables, 7 refs.
Unclassified Report

The Dynamic Test Method has been successfully applied for obtaining core fatigue in shear by reversed bending of a double cantilever beam sandwich specimen containing heavy tip-end masses. The testing approach consists of applying forced vibrations at resonant frequency with an electromagnetic shaker for each stress level desired.

1. Sandwich construction
2. Fatigue testing
3. Test method
I. AFSC Project 7381, Task 738103
II. Contract AF 33 (657)-7309
III. Northrop Corp. Norair Div. Hawthorne, Calif.
IV. D. R. Apodaca
J. L. Preston
V. Secondary Rpt No. NOR 63-25
VI. Not aval fr OTS
VII. In ASTIA collection

Aeronautical Systems Division, Dir/Materials and Processes, Applications Lab, Wright-Patterson AFB, Ohio.
Rpt Nr ASD-TR-61-338, Part II. FATIGUE IN SHEAR BY BENDING OF STRUCTURAL SANDWICH CONSTRUCTIONS. Final report, Mar 63, 45p. incl illus., tables, 7 refs.
Unclassified Report

The Dynamic Test Method has been successfully applied for obtaining core fatigue in shear by reversed bending of a double cantilever beam sandwich specimen containing heavy tip-end masses. The testing approach consists of applying forced vibrations at resonant frequency with an electromagnetic shaker for each stress level desired.

1. Sandwich construction
2. Fatigue testing
3. Test method
I. AFSC Project 7381, Task 738103
II. Contract AF 33 (657)-7309
III. Northrop Corp. Norair Div. Hawthorne, Calif.
IV. D. R. Apodaca
J. L. Preston
V. Secondary Rpt No. NOR 63-25
VI. Not aval fr OTS
VII. In ASTIA collection

Reliable and reproducible S-N fatigue curves were produced on adhesive-bonded aluminum alloy and brazed stainless steel specimens containing representative shear test areas. Cell geometry and bond quality were found to significantly affect fatigue life of this material.

Reliable and reproducible S-N fatigue curves were produced on adhesive-bonded aluminum alloy and brazed stainless steel specimens containing representative shear test areas. Cell geometry and bond quality were found to significantly affect fatigue life of this material.

Reliable and reproducible S-N fatigue curves were produced on adhesive-bonded aluminum alloy and brazed stainless steel specimens containing representative shear test areas. Cell geometry and bond quality were found to significantly affect fatigue life of this material.

Reliable and reproducible S-N fatigue curves were produced on adhesive-bonded aluminum alloy and brazed stainless steel specimens containing representative shear test areas. Cell geometry and bond quality were found to significantly affect fatigue life of this material.